A guide to lithostratigraphy and structural inventory of the Cycladic Blueschist Unit rocks of NE Attica (Greece)

Lozios S., Soukis K. and Antoniou V.

Journal of the VIRTUAL EXPLORER, Electonic Edition, ISSN 1441-8142, volume 50, Paper 3, DOI: 10.3809/jvirtex.2016.08691, In: (Eds) Adamantios Kilias and Stylianod Lozios, Geological field trips in the Hellenides, 2019.

Journal of the VIRTUAL EXPLORER

A dynamic review electronic Earth Science journal publishing material from all continents

A guide to lithostratigraphy and structural inventory of the Cycladic Blueschist Unit rocks of NE Attica (Greece).

Lozios S.[1]*, Soukis K and Antoniou V.*

[1] National and Kapodistrian University of Athens, Department of Geology and Geoenvironment, GR-15784, Athens, Greece.

GUIDE INFO

Keywords
Hellenides, NE Attica, Lithostratigraphy, micro- and macro-scale structures, structural evolution

Citation
Lozios S., Soukis K. and Antoniou V., 2019. A guide to lithostratigraphy and structural inventory of the Cycladic Blueschist Unit rocks of NE Attica (Greece). Journal of the Virtual Explorer, Electronic Edition, ISSN 1441-8142, volume 50, paper 3. doi: 110.3809/jvirtex.2016.08691.

Correspondence to:
slozios@geol.uoa.gr

IN THIS GUIDE

NE Attica, the area between Pentelikon Mt. and Southern Evoikos Gulf (Fig. 1), represents the northwestern prolongation of Attic-Cycladic Crystalline Complex (ACCC). It consists of metamorphic rocks equivalent to those of Southern Attica, Southern Evia and the Cyclades. A small amount of research has been carried out in Attica and even less in NE Attica. Most researchers accept the geotectonic scheme given by Marinos & Petrascheck (1956) for the area of Lavrion (Southern Attica), which comprises a relative autochthonous tectonic unit (Lower Unit) and an overlying allochthonous Phyllitic Nappe (Upper Unit). Recent publications (e.g. Katsikatsos et al. 1986, Photiades & Carras 2001, Skarpelis et al. 2008, Liati et al. 2009, Baziotis et al. 2009, Krohe et al. 2010, Spanos et al. 2010, Xypolias et al. 2010, Baziotis & Mposkos 2011, Liati et al. 2013, Baziotis et al. 2019) correlate the Lower Unit with the Basal Unit and the Upper Unit with the Cycladic Blueschist Unit (CBU). The aim of this field-guide is to: i) propose a new refined lithostratigraphy of NE Attica, ii) present a geological map in scale 1:25.000, iii) present new structural and petrographical data for the structural evolution of this part of the ACCC and iv) propose two one-day field trips (from Pentelikon Mt. up to the coastal zone of Southern Evoikos Gulf) that will shed light both to the NE Attica lithostratigraphy and macrostructure of the Lower and Upper units as well as the main structures formed mainly during the retrograde path. The stops of the two, one-day, excursions and the geological map in scale 1:25.000, are also given online, as .kmz (Field-trip.kmz) and .pdf (Geological Map.pdf) files respectively.

INTRODUCTION

In the first part of this guide we discuss the geological structure and tectonometamorphic evolution of the NE Attica units, as they have been presented in the few published papers and correlate them with the available data from Southern Attica and the Cyclades. Though it is certain that both units have undergone HP metamorphism, followed by a greenschists facies event, there are still many questions concerning: (i) the correlation of the tectonic units with those known from the Cyclades, (ii) the representative lithostratigraphic columns, (iii) the age and the protolith of the metamorphic rocks and (iv) the exact timing of metamorphism, the structural evolution and the exhumation history. In this work new lithostratigraphic and structural data and a new 1:25.000 scale geological map are presented, aiming to address some of the above mentioned.

In the second part, the proposed lithostratigraphy for NE Attica, as this was deduced by the geological mapping, the field observations and structural analysis of meso and macroscopic scale structures, is presented in selected outcrops. Additionally, representative structures that highlight the structural relationships and overprinted foliations as well as kinematic indicators, are shown and analyzed. Finally, these data are integrated with existing petrological and P-T data and so that the tectonometamorphic evolution of the geological units is eventually revealed.

GEOLOGY OF ATTICA

Attica can be divided in two parts. The northwestern part is occupied by the upper-plate non- to very low-grade metamorphosed formations of Sub-Pelagonian Unit. The eastern and southeastern part comprises lower plate metamorphic rocks , that represent the NW part of Attic-Cycladic Crystalline Complex (ACCC). The contact between those two domains is covered by the Neogene formations of Athens–Agios Stefanos–Kapandriti Basin (Fig. 1). Along the margins of the ACCC and within the basin, two more tectonic units can be observed: the very low grade Alepovouni Unit that covers tectonically the NW margin of ACCC, and the mélange type "Athens Schists", which tectonically overlies both the SE margin of the Sub-Pelagonian Unit as well as the NW margin of the ACCC and the Alepovouni Unit (Lekkas & Lozios 2000, Papanikolaou et al. 2004a, 2004b).

Most people accept the tectonostratigraphic column of Attica that Marinos & Petrascheck (1956) proposed for Lavrion peninsula, which includes a Lower and an Upper Unit. The Lower Unit comprises a Lower and an Upper Marble and a schist formation, with a blue-grey metachert marble layer in between, known as the Kessariani Schists. The base of the Lower Marble is partially dolomitic and/or with distinctive schist layers. Lekkas & Lozios (2000) identified a low-angle fault in Hymittos Mt. that juxtaposed the dolomitic lower part against the overlying calcitic part of the Lower Marble. So, they proposed that this lower part constitutes a different unit (named as Vari-Kirou Pira Unit). The Upper Unit represents a more heterogenous formation including schists, quartzite, blocks of mafic and ultramafic rocks and a thicker marble sequence at the top.

Most researchers correlate the Lower Unit with the Basal Unit known from Olympus Mt., Southern Evia, and Samos Island and the Upper Unit with the Cycladic Blueschist Unit (CBU, Katsikatsos et al. 1986, Lozios 1993, Skarpelis 2007, Skarpelis et al. 2008, Baziotis et al. 2009, Liati et al. 2009, Krohe et al. 2010, Spanos et al. 2010, Xypolias et al. 2010, Baziotis & Mposkos 2011, Berger et al. 2013, Scheffer et al. 2016). There are also publications which do not exclude that both units (Lower and Upper) are different parts of the CBU, based on lithostratigraphic, structural, petrological and geochronological data and correlations between Attica, Cyclades and S. Evia, (Lozios 1990, 1993, Kessel 1990, Shaked et al. 2000, Lekkas et al. 2011, Liati et al. 2013, see also comments below).

The contact between the Lower and Upper unit was initially considered to be a thrust (Marinos & Petrascheck, 1956, Katsikatsos et al. 1986, Katsikatsos 2002). During the last two decades several researchers describe low-angle normal faults juxtaposing the two units as well as within each unit, resulting in significant changes to the tectonostratigraphy of Attica (Lekkas & Lozios 2000, Photiades & Carras 2001, Papanikolaou et al. 2004b, Krohe et al. 2010, Lekkas et al. 2011, Scheffer et al. 2016). This is in accordance with structural observations in Western Cyclades, where a series of low-angle normal faults constitute the Western Cycladic Detachment System (WCDS), a crustal-scale detachment system, that seems to prolongate to SE Attica (Iglseder et al. 2011, Lekkas et al. 2011, Grasemann et al. 2012, Seman et al. 2012, Seman et al. 2013, Scheffer et al. 2016).

GEOLOGY OF NE ATTICA

The area of NE Attica is bordered by Southern Evoikos Gulf (North and East), Athens basin and Hymmitos Mt. (South) and Agios Stefanos–Kapandriti basin (West - Fig. 1). The pre-Miocene basement of NE Attica consists of HP metamorphic rocks, which can be subdivided in two tectonic units, a lower and an upper one, consisting of marble, schists with distinctive blue-grey or metachert marble layers, quartzite, metabasite, acid metavolcanics and sparse serpentinite blocks (Lozios 1990, 1993, Kessel 1990, Katsikatsos 2002, Krohe et al. 2010, Xypolias et al. 2010, Baziotis et al. 2004, 2019). The lower NE Attica Unit (NEAU, Lozios 1990, 1993), occupies most of the mountainous area from Penteli Mt. to Southern Evoikos Gulf. In contrast, the upper Agios Georgios Unit (AGU, Lozios 1990, 1993), appears in the form of relic outcrops along the eastern margin of Agios Stefanos–Kapandriti basin, mainly in the area close to the artificial Marathon Lake (Fig. 1).

There are lithological differences between the two units but the significant difference is in the P-T paths. The dominant foliation of NEAU is formed by typical greenschist facies mineral assemblages. HP minerals are only found as relict inclusions in albite (see Fig. 8d / Stop 1.1). On the contrary, blue amphiboles in AGU are abundant (see Fig. 23a&b / Stop 2.2) and glaucophane is a well-preserved mineral forming the main foliation (Lozios, 1993). According to Baziotis et al. (2019), the NEAU underwent a HP/LT metamorphic

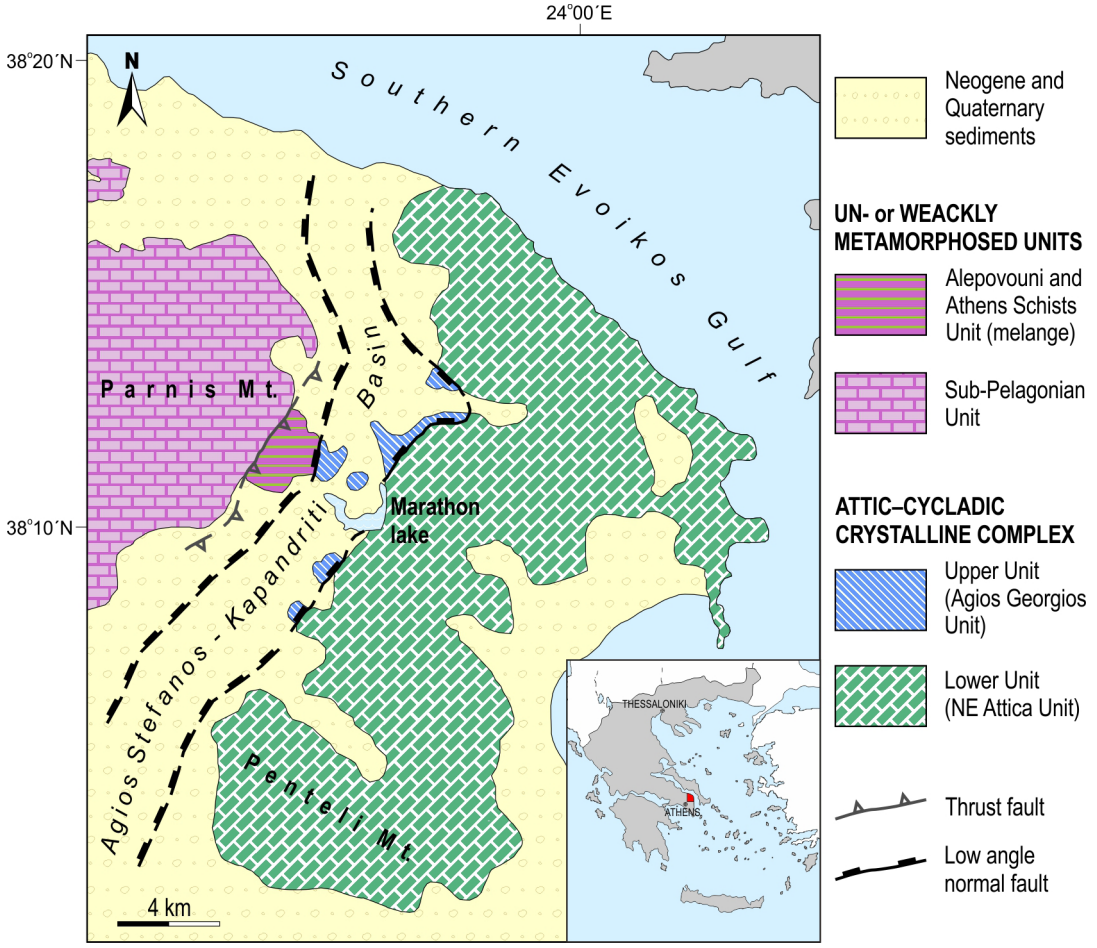

Figure 1
Simplified geological map of NE Attica, showing the main units.

event with a P-T peak at 9-11 kbar and ~370 °C, followed by decompression at 5-6 kbar and a temperature increase during the exhumation, leading to the strong overprint of blue amphiboles by the greenschist mineral assemblages. A different P-T path is given from the same author for the AGU, where mineral assemblages in metabasic rocks record a HP/LT event with a lower P-T peak at ~9 kbar and ~350–370 °C, followed by continuous cooling during the exhumation. It is pointed out that although P-T conditions for NEAU are similar with those of the Basal Unit in Evia (Shaked et al. 2000) the P-T path is different since the latter is characterized by decompression cooling.

INTERPRETATION OF LITHOSTRATIGRAPHY

The lithostratigraphic sequence of the Lower Unit in Southern Attica, is also applicable for NEAU, mainly for the Penteli Mt. metamorphic rocks. This includes a lower marble at the base, an intermediate of schist layer and an upper marble at the top. But examining the whole area all the way to the North and up to the coastal zone of Southern Evoikos Gulf, at list three thick marble layers are identified, alternating with three (also thick) schist layers are identified. It is debated whether this successive repetition of marble and schists corresponds to different stratigraphic layers or there is a simple stratigraphy, which includes a marble and a schist alternating due to isoclinal macro-scale folding, or imbricate thrusts (Lozios 1993, Kessel 1990, Katsikatsos 1992, Spanos 2012). The existence of a geological and structural map accompanied by structural analysis of the complicated macro-folds, is necessary to depict the stratigraphic relationship between the marble and schist sequences. For this reason, a 1:25.000 map of the NE Attica metamorphics, modified after Lozios (1993), accompanies this field guide, available also on-line.

Based on: i) detailed geological mapping in 1:25.000 and 1:5.000 scale in selected areas and identification of the existing macro-scale fold

hinges, mainly through the blue-grey marble marker layer (see Fig. 12 / Stop 1.3, Fig. 17 &18 / Stop 1.7 and Fig. 27 / Stop 2.5), ii) detailed structural analysis of 1st and 2nd order macro-scale folds, using fold geometry, fold asymmetry and vergence, iii) the existence of the same marker layers (e.g. the blue-grey marble near the marble/schist contacts) both in normal and overturned limbs of the macrofolds (see Geological Map), iv) the ages given by the rare fossils found in the marble (Fig. 2) and v) the petrological and petrographical characteristics and the field relations between the various lithologies, Lozios (1993) suggested that the present lithostratigraphy is the result of isoclinal macro-scale folding and the original stratigraphic column is very simple including a meta-volcanosedimentary sequence at the base overlain by a meta-carbonate platform (neritic marble sequence in Fig. 2).

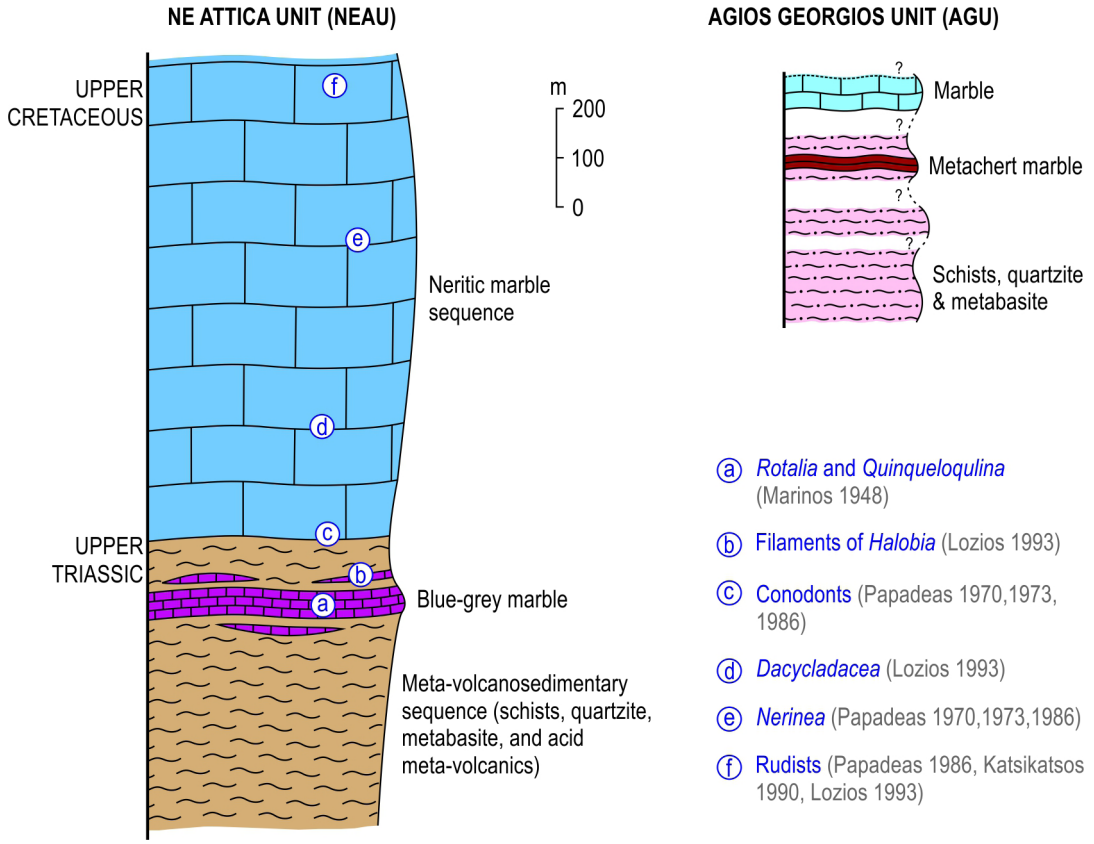

Figure 2
Representative litho-stratigraphic columns of the underlying NE Attica Unit (NEAU) and the overlying Agios Georgios Unit (AGU).

The basal meta-volcanosedimentary sequence has a thickness that varies from few hundred to more than 12 hundred meters and comprises various lithologies such as schists, quartzite, metabasite and acid meta-volcanics. At the upper part of the meta-volcanosedimentary sequence a prominent blue-grey (and/or white or metachert) marble exists, which represents the transition to the marble sequence (Fig. 2). Usually, in the field one can observe the alternation between the above mentioned lithologies, with a thickness that varies from few centimeters to hundreds of meters (see Fig. 9 / Stop 1.2). The coexistence of acid metavolcanics and metabasite, which is common for the mid Triassic sequences in the Hellenides, is an evidence of bimodal magmatism (Pe-Piper & Piper 2002). This is also supported by the ages obtained from rare fossils in the marble (see next paragraph) and is in accordance with the lithostratigraphy of the CBU (Lozios 1993). The presence of metagranitoids, in the form of strongly elongated lenses (tens or hundreds of meters long) within the lower formation of NEAU in Penteli Mt., are reported by Kessel (1990), Lozios (1993) and Liati et al. (2013). U–Pb SHRIMP zircon geochronological data and zircon morphology strongly indicate an I-type pluton origin with two successive stages of crystallization, at 255±3 Ma and 246±2 Ma, and a rift-related geotectonic setting, similar to CBU (Liati et al. 2013).

The marble sequence consists of white, grey or

blue thick to medium bedded marble and it has a thickness that varies from 500 to more than 1.000 m. In many cases, near the contact with the lower formation, the marble sequence passes to a blue or grey marble with abundant thin layers of metacherts, schists, metabasite or acid meta-volcanics. The main features of the marble (color, composition, thickness etc.) vary from place to place as expected in a carbonate sequence that was folded isoclinally in the macroscale. The age is partially constrained since sparse fossils have been found within the marble (Marinos 1948, Papadeas 1970, 1973, 1986, Katsikatsos 1990, Lozios 1993). Badly preserved fossils found at the basal layers of the overlying marble and within the transitional beds to the underlying meta-volcanosedimentary sequence, indicate a Late Triassic age. The uppermost part of the marble has a late Cretaceous age and all the fossils found in the marble sequence suggest a neritic depositional environment. Hence, the marble sequence represents a neritic carbonate platform, ranging from the late Triassic to late Cretaceous, and consequently a Late Triassic or older age can be assumed for the meta-volcanosedimentary sequence (Fig. 2).

Due to limited exposure and severe faulting there is not enough data to construct the lithostatigraphic column of AGU. The main outcrop occupies the area west of the Marathon reservoir (Fig. 1), and includes a sequence of: i) Na-amphibole schists, quartzite and metabasic blocks (rich in Na-amphibole), of about 500 m thickness, at the base, ii) a prominent dark metachert marble layer and iii) less than 100 m thick white - grey marble at the top (Fig. 2). It should be noted that the lithological types, petrology and field-relations are almost identical with those of the Upper Unit in Southern Attica (Lozios 1993).

The tectonic contact between NEAU and AGU is almost everywhere covered by Neogene sediments and can be only observed north of the Marathon reservoir (Fig. 1). It is an NNE fault dipping moderately (45°-50°) WNW (see Fig. 22 / Stop 2.2) and juxtaposes the NEAU marble (footwall) against the Na-amphibole schists of AGU (hanging wall). Preserved dip-slip slickenlines on the fault surface reveal that it is a normal fault. The fault core shows only cataclastic deformation along the fault surface, developed on the roof of NEAU marble, which is spatially associated with massive fluid infiltration and extensive alteration (ankeritization). The fault-rock is composed of a 5-40 cm zone of tectonic breccia, developed along the footwall marble and a wider zone (up to 2-3 m) containing angular to lensoid clasts (quartzite and dark marble), originating mostly from the hanging wall rocks. Rare kinematic data, mainly shear-bands or flanking structures, indicate a top-to-WSW sense of shear.

STRUCTURAL DATA

Structural observations in NEAU and AGU, combined with geological mapping and the resulting macro-scale structures, reveal the structural evolution of the NE Attica metamorphic rocks. Based on structural analysis and cross-cutting relationships, five deformation events can be distinguished that progressively took place from ductile to brittle conditions during the exhumation path of the HP rocks.

Dn-1 and Dn

The oldest event that can be identified in NEAU, is the Dn-1 event, associated with the HP metamorphism, as indicated by the presence of relict Na-amphibole inclusions in albite and epidote porphyroblasts of the dominant greenschist facies Dn event. These inclusions constitute the trace of the Sn-1 foliation (see Fig. 8h / Stop 1.1). The mineral assemblages and the structures of Dn-1 have been totally obliterated by the greenschist facies overprint. The Dn event, is associated with the greenschist facies metamorphic event during the early stages of exhumation. The dominant coarse-grained foliation Sn represents a penetrative structure that can be observed in all lithological units. It is formed by the strong alignment of greenschist facies minerals such as chlorite, epidote, actinolite, albite as well as quartz, micas, calcite etc. A well-developed Ln mineral, stretching and/or intersection lineation formed along with the main foliation. It has a relatively constant NE-SW direction (from N050° up to N070°), and it plunges towards NE or SW (Fig. 3), due to subsequent Fn+1 folds (see below).

The syn-metamorphic Fn folds appear as isoclinal to very tight recumbent folds and the Sn constitutes the axial planar foliation to these folds. They mostly have the same orientation as the Ln stretching lineation (Fig. 3), but locally they display significant variations, due to intense deformation and fold axes re-orientation into parallelism with the Ln (non-cylindrical sheath folds, see

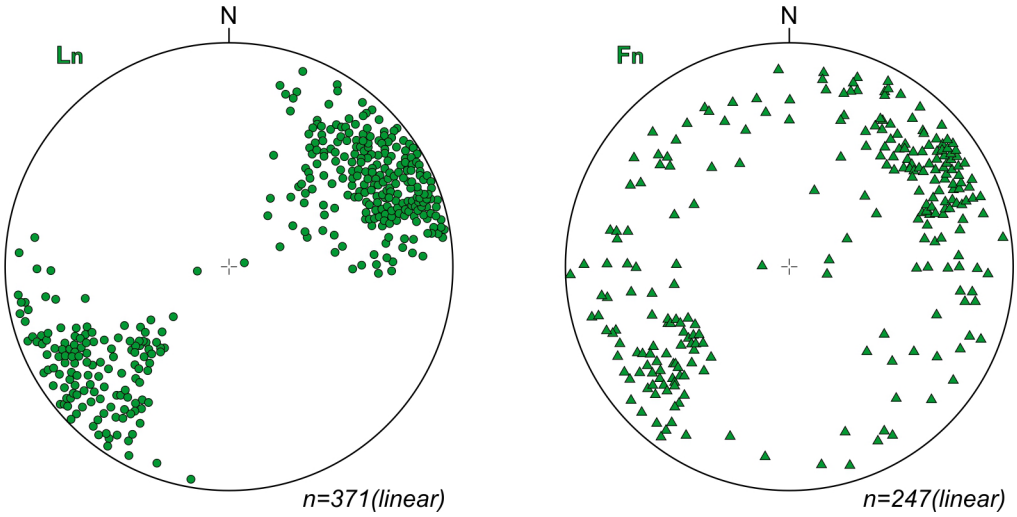

Figure 3
Equal-area, lower hemisphere projections of the Ln mineral, stretching and/or intersection lineation and the Fn isoclinal fold axes.

Fig. 14c&d / Stop 1.5). They are easily observed in metachert marble or in blue-grey marble layers and just like the Ln they form two-point maxima in a stereo-plot projection: one dipping to NNE and another to WSW, only in this case the Fn axes are more scattered but symmetrically arranged on both sides of the dominant NE-SW trend of the Ln. The Fn folds can be observed in all scales, leading to the successive alternations between the upper meta-carbonate and the lower meta-volcanosedimentary part of NEAU lithostratigraphic column. In some areas two or more successive events of co-axial re-folding during Dn have been identified, thus giving successive NE-SW isoclinal recumbent folds in cm- to dm-scale (e.g. metachert marble, see Fig. 25a / Stop 2.3), and even to several 100-m-scale (e.g. the blue-grey marble layer, see Fig. 12 / Stop 1.3).

In many cases the foliation appears to be mylonitic, mostly within the marble or the meta-tuffs and the acid meta-volcanics. Strain partitioning during the Dn event is probably responsible for this higher strain gradient within these ten to hundred meters thick mylonitic zones, where a strong NE-SW stretching lineation and NE-SW sheath- or intrafolial-folds are very common (see Fig. 25a / Stop 2.3). The sense of shear is mostly top to SW - WSW, but rarely a top to NE shear sense can be also observed.

In AGU, the dominant Sn foliation includes mainly the minerals of the HP metamorphic event (e.g. glaucophane and lawsonite) since this unit is characterized by continuous cooling during the exhumation and only partially the glaucophane is replaced by actinolite. Hence, for AGU, the Sn and Sn+1 foliations of NEAU are identical. The NE-SW Ln mineral and/or stretching lineation is also very common in the marble or schists of AGU, while Fn folds were hardly detected.

Dn+1

For both units, the semi-brittle structures formed during the Dn+1 event include folds, spaced foliations and intersection/crenulation lineations. These structures record the transition to the post-metamorphic stage during the exhumation path. The Fn+1 folds are very common and can be observed in all scales. During this event all the Dn structures have been folded by NW-SE to N-S folds (Fig. 4, see also Fig. 1). Several types and fold-geometries characterize this event, including cylindrical (and rarely slightly curved non-cylindrical) open to tight folds, chevron or box-folds and upright or usually asymmetrical inclined folds (with NE or rarely SW vergence) which in some cases are accompanied by an Sn+1 axial planar crenulation cleavage (see Fig. 11 / Stop 1.3 and Fig. 25c&d / Stop 2.3). Lithology, strain partitioning, timing of deformation (early or late structures during this event) are responsible for this diversity.

The Sn+1 foliation associated with the Dn+1 event has formed as axial planar foliation to the Fn+1 folds and it is penetrative only locally. In the more competent layers, such as marble or acid meta-volcanics, only a widely spaced cleavage in the highly strained fold hinges can be observed. On the contrary, within the schists and to a lesser degree in the blue-grey marble, a few meters to hundreds of meters wide zones, with a densely spaced crenulation cleavage are developed. In these cases, the folded schistosity Sn is strongly overprinted by the spaced cleavage Sn+1 but the

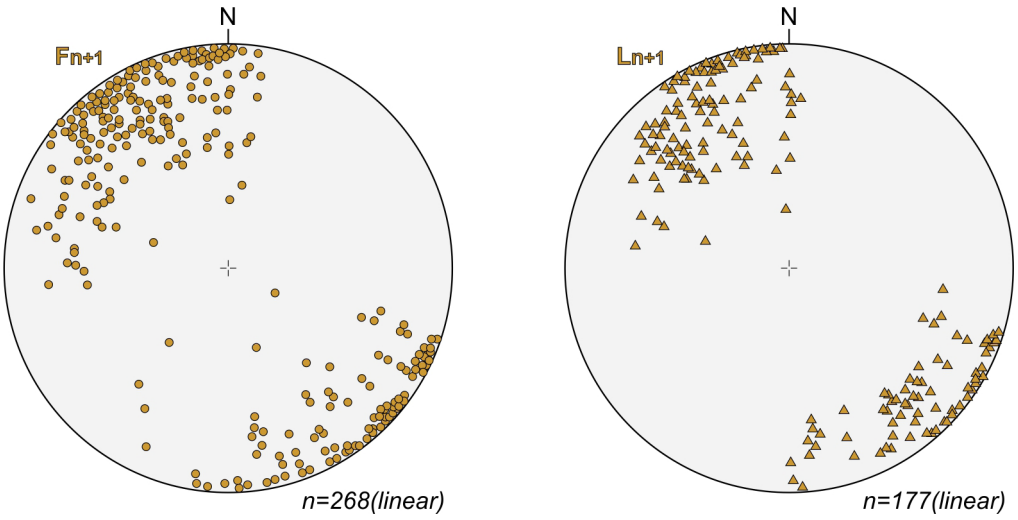

Figure 4
Equal-area, lower hemisphere projections of the Fn+1 open to tight fold axes and the Ln+1 intersection and/or crenulation lineation.

microlithons remain visible (see Fig. 30a-f / Stop 2.7). The mineral assemblages of Sn are usually bent and reoriented or fractured along the subsequent Sn+1 cleavage. At the early stages of this event and at the deeper levels of the lithostratigraphic column (Penteli Mt. area) and probably in high strain zones, small scale dynamic recrystallization of minerals such as quartz, white-micas and chlorite occurs along the cleavage domains (see Fig. 19 / Stop 1.8). The cleavage planes usually dip moderately to steeply (40°-60°) towards NE-E, although there are places (mainly along the western part of the area and near the contact with the AGU) where the cleavage planes are dipping NW-W and rarely N. It should be noted though that the vergence of the Fn+1 folds remains in most cases to SW. The dominant linear structure of Dn+1, event is represented by an Ln+1 crenulation or Sn-Sn+1 intersection lineation with identical orientation to the Fn+1 fold axes (NW-SE to N-S, Fig. 4). The structures of Dn+1 event seem to have a compressional character and top-to-SW sense of shear, showing a NE-SW to ENE-WSW horizontal shortening, similar to the previous syn-metamorphic Dn phase.

Dn+2

The Dn+2 event is characterized by semi-brittle to brittle extensional structures, such as shear-bands or complex small-scale faults, that deform both the dominant Dn schistosity and the Dn+1 cleavage (see Fig. 30g / Stop 2.7). Although these structures are relatively sparse, they can be found throughout the area. The sense of shear is mostly top-to-NE - NNE but top to SW can be also observed, mainly along the contact between NEAU/AGU, indicating a NE-SW to NNE-SSW horizontal extension.

Dn+3

The Dn+3 event is characterized by cataclastic deformation and it is associated with NW-SE high-angle normal faults observed in all scales. They show a dominant NW-SE direction (similar to the neotectonic basin of Southern Evoikos Gulf) and a dip direction both to NE as well as to SW, forming typical horst and graben structures. The fault zone along the NE border of Penteli Mt. and the fault zones along the coast of Southern Evoikos Gulf are the most representative (see Fig. 26 / Stop 2.4 and the Geological Map). A thick zone of cohesive to non-cohesive cataclasites (tectonic breccia or microbreccia), slickensides and dip-slip slickenlines are common along the fault surfaces. Morphological features, such as triangular facets, linear erosion, fault scarps and scree and talus cones, suggest that these faults are active and operating under NE-SW extension, and the seismological data from the submarine seismic faults of Southern Evoikos Gulf (e.g. Oropos 1938, M=6.0 and 1986, M=4.4 earthquakes) seem to confirm this. In some places a series of parallel mesoscopic scale faults, dipping 40°-50° towards SW, can be observed, with a throw of no more than 10 meters. A simple shear domino model can be applied locally for these cases instead of the pure shear horst and graben model for the macroscale fault zones.

FIELD GUIDE

The two, one-day, excursions include roughly E-W transects along the southern, central and northern part of the area and they are arranged from south to north. The first day covers the geology and structure along the southern and northern slopes of Penteli Mt. and the second day the geology and structure of the central (from Marathon Lake to Kato Souli and Ramnous archaeological site) and northern part (Varnavas village) of NE Attica.

The Stop locations are shown on the simplified geological map of Fig. 5, as well as on the Google Earth image of Fig. 6. They are also available on-line as kmz files (Field-trip.kmz). The WGS 84 is used as the coordinate system, as it is common in Google Earth and most of the on-line maps.

The orientation measurements are given as dip direction/dip angle and plunge direction/plunge angle for planar and linear structures respectively.

It goes without saying that we do not hammer or destroy the structures (not only those shown in photographs), so that they will be available for all geologists and for student field education.

Excursion 1: Southern and northern flanks of Penteli Mt.

This excursion includes five short walks and several point observations along foot paths and dirt or asphalt roads. The rock types of NEAU, the possible protoliths, the lithostratigraphy and the tectonic structures in micro and macro-scale are shown, described and discussed.

Stop 1.1.a-c: The meta-volcanosedimentary sequence and the Dn structures of NEAU.
(1.1.a) 38°03'46"N, 23°52'32"E
(1.1.b) 38°03'46"N, 23°52'30"E
(1.1.c) 38°41'24"N, 23°52'35"E

The outcrop locations of Stops 1.1 and 1.2 as well as characteristic locations mentioned in the text, are shown on a Google Earth image in Fig. 7.

The first order crest of Penteli Mt. has a NW-SE direction. The second order morphological axes (crests, main streams and valleys) on the southern cliffs of the mountain, dips to the SW, just as the Dn linear structures and macro-stractures (Fn isoclinal recumbent macro- and micro-fold axes and Ln stretching lineation). The result of it is the successive NE-SW elongated alternations between the main lithological types of NEAU that can be easily observed in the field (Fig. 8a).

In Fig. 8a, a huge layer of marble can be seen, which corresponds to the lower part of the NEAU neritic marble sequence (see Fig. 2). Many marble quarries can be easily recognized along this layer, which are currently inactive due to the environmental impacts of quarrying. These quarries have been operating since the ancient times of the city of Athens, from where the famous "Pentelikon white marble" was mined. From this marble several memorable monuments and sculptures have been constructed, such as the Parthenon, the Erechtheum and the Propylaea on the Acropolis of Athens.

From Palaia Penteli Square drive towards the 414 Military Hospital, until the end of Spilias Street. Then walk along the Hospital fence, up to the Stop 1.1.a (Fig. 7). In this stop NE-SW elongated outcrops of meta-tuffs can be observed, dipping slightly to the west (Fig. 8b). The dominant Sn schistosity is formed by the typical greenschist facies minerals and demonstrates a mylonitic character. So, 1-2 mm porphyroclasts of albite (and rarely epidote or quartz), within an anastomosing foliation formed mainly by muscovite and chlorite, represents the main picture in the field. The presence of σ-type clasts, in sections parallel to the NE-SW Ln stretching lineation, shows a top-to-SW movement (Fig. 8c), but the opposite can be also observed. Vertical joints, perpendicular to the Sn main schistosity and Ln stretching lineation, form typical fringe zones, where a series of twist hackles arranged en echelon, due to local changes of stress orientation (Fig. 8d).

Some meters to the west, at Stop 1.1.b (Fig. 7), along linear outcrops of meta-tuffs, isoclinal, recumbent, meter- to tens of meters-scale Fn folds can be observed, trending mainly NE-SW (Fig. 8e). The minerals of the Sn foliation are arranged parallel to the axial planes and the older foliation, which is isoclinally folded, corresponds to either the Sn-1 foliation or an early stage of the Sn. Where observed, the Sn-1 is parallel to the dominant Sn, defining a composite Sn-1/n foliation. Only in cases where an internal fabric, formed by straight Na-amphibole inclusion trails, is preserved in albite (or epidote) porphyroblasts, the Sn-1 is oblique to the external Sn foliation (Lozios 1993). A prominent NE-SW stretching lineation (Ln) growing on Sn surfaces, along which the quartz, albite and other greenschist minerals are strongly elongated (Fig. 8f).

Walking to Stop 1.1.c we crosscut successive

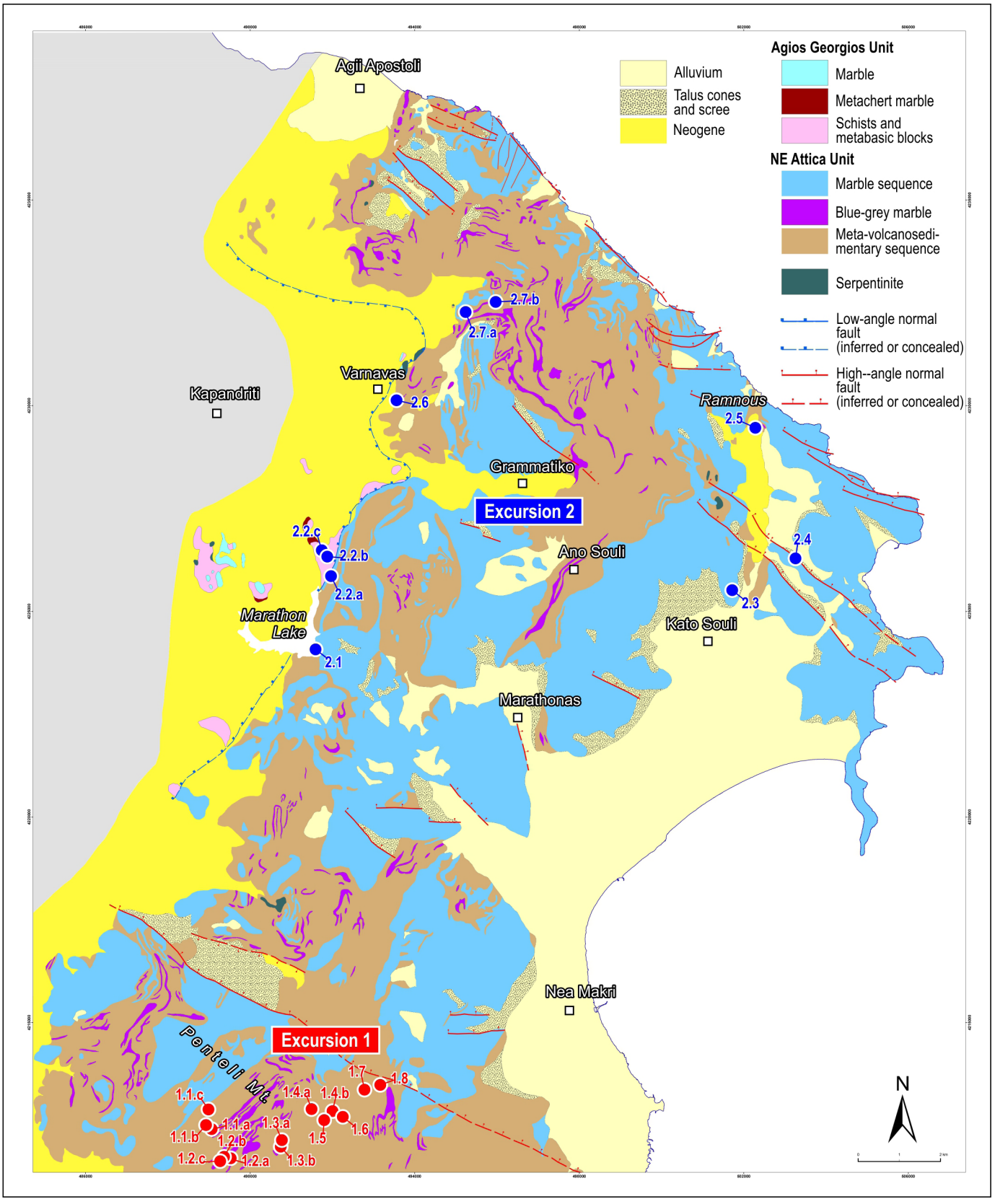

Figure 5
Simplified Geological map showing the location of the Stops where important outcrops are described in the Field Guide.

Figure 6
The Stops locations on a Google earth image, during the two, one day, excursions.

NE-SW alternations of schists, metabasite, acid meta-volcanics, quartzite and thin layers of blue-grey marble. The most representative mineral assemblages for these rocks that characterize the meta-volcanosedimentary sequence at the base of NEAU, include: – Metabasite: actinolite + epidote + chlorite + albite + titanite macmuscovite ± biotite quartz ± garnet ± hornblende ± pyroxene ± calcite ± potassium feldspar (blue amphibole as inclusions in albite and epidote, Fig. 8h) – Acid meta-volcanics: quartz + albite + muscovite ± chlorite ± biotite ± titanite ± epidote ± calcite (Fig. 8i) – Quartzite: quartz + albite ± chlorite ± muscovite ± biotite ± epidote – Schists: quartz + muscovite + biotite + chlorite ± albite ± epidote

Figure 7
Location of Stops 1.1 and 1.2 on a Google Earth image.

(Fig. 8j).

At Stop 1.1.c (Fig. 7), the underlying basic meta-lavas of the meta-volcanosedimentary basal sequence, alternate with the overlying white marble, of the lithostratigraphic column of NEAU (Fig. 8g). Noted that in other places the marble is in contact with both the schists and the acid meta-lavas or the meta-tuffs.

Stop 1.2.a-c: The blue-grey marble and the Dn and Dn+1 structures of NEAU.
(1.2.a) 38°03'20"N, 23°52'52"E
(1.2.b) 38°03'56"N, 23°52'97"E
(1.2.c) 38°03'19"N, 23°52'44"E

From Spilias Street drive towards Nea Makri town up to the Stop 1.2.a (Fig. 7), where a layer of blue-grey marble, with a thickness of about 120 meters, appears (Fig. 9a), dipping gently to WSW (Sn 258/18). On the Sn foliation planes a strong stretching lineation, slightly plunging towards NE can be also observed (Ln 044/14, Fig. 9b). About 70 meters to the west, at Stop 1.2.b (Fig. 7), another blue-grey marble thick layer (~70 meters) is intercalated within the metabasite and acid meta-volcanics (Fig. 9c). The Sn main schistosity dips 222/25 but the Ln stretching lineation remains stable at 228/24 (Fig. 9d). These two blue-grey marble layers are the same layer, which is repeated due to isoclinal folding of the Dn deformation event (see also Stop 1.3).

At Stop 1.2.c (Fig. 7), two transverse lineations can be observed on the Sn foliation surfaces (dipping 100/25) of a meta-tuff outcrop (Fig. 9e). The Ln stretching lineation (052/18) is deformed by the Fn+1 micro knicks (150/16) of the last stages of Dn+1 phase (Fig. 9e). In sections normal to Sn main foliation, which in this outcrop demonstrates a mylonitic character, and parallel to Ln stretching lineation, σ-type porphyroclasts and shear bands show a top-to-SW sense of shear (Fig. 9f).

Stop 1.3.a & b: The Fn+1 refolding, the Sn+1 axial-planar cleavage development and the Fn recumbent macro- folds of the blue-grey marble of NEAU.
(1.3.a) 38°03'35"N, 23°53'48"E
(1.3.b) 38°03'36"N, 23°53'16"E

The outcrop locations of Stops 1.3 up to 1.6 as well as characteristic locations mentioned in the text, are shown on a Google Earth image in Fig. 10.

Continue driving on the asphalt road to Nea Makri. Park at the beginning of the dirt road that leads to the Stop 1.3.a and walk up to that point. On the road surface mesoscopically refolded chlorite-epidote schists and acid meta-volcanics are exposed. The Fn+1 open to tight folds refold the Sn main schistosity and the Fn isoclinal folds, in which an earlier foliation (Sn-1 or early stage Sn) is isoclinaly folded (Fig. 11). A dense Sn+1

Figure 8
The lithological types of the meta-volcano-sedimentary sequence and the Dn structures of NEAU..

Figure 9
The blue-grey marble within the meta-volcanosedimentary sequence of NEAU and the Dn and Dn+1 structures of NEAU.

axial-planar cleavage has been developed, which is overprinting the earlier Dn structures. Cleavage fanning is observed between layers with high competence contrast and hence the Sn+1 cleavage planes are densely spaced in layers rich in phyllosilicates whereas in the more competent quartzitic layers they are much less frequent (Fig. 11). The Fn and Fn+1 fold axes that exposed due to the road-cut (in oblique section to both of them) are almost perpendicular to each other, dipping 042/36 and 305/26 respectively and forming type 3 interference patterns associated with refolding of Fn isoclinal folds around Fn+1 folds (Ramsay, 1967). Alternating class 1B and 3 folds (Ramsay 1967) can be also seen in the folded layers (see the central and the upper part of the fold), so as to accommodate overall deformation. The competent layers exhibit class 1B geometry while the less competent exhibit class 3.

Continue walking up to the Stop 1.3.b, on top of the hill. Looking towards the west the blue-grey marble layer within the meta-volcanosedimentary sequence is isoclinaly folded forming a large scale subhorizontal recumbent Fn fold. The fold hinge (Fig. 12a) trends NE-SW and the axial plane is shallowly dipping towards the WSW. This marble layer can be traced all over this area as four distinct parallel layers that join in the hinges of recumbent isoclinal macro-folds (synforms or antiforms). Geological mapping and detailed

Figure 10
Location of Stops 1.3 up to 1.6 on a Google Earth image.

structural analysis (fold asymmetry and vergence) revealed at least three NE-SW co-axial isoclinal refolding stages [Fn(1), Fn(2) and Fn(3), Fig. 12b) that form type 3 interference patterns (Ramsay 1967). The axial plane traces of these isoclinal folds (Fig. 12c) clearly illustrate the superposition of the three successive isoclinal refolding events.

At Stop 1.4.a right at the beginning of the dirt road, there is a layer, which is rich in late- to post-tectonic pyrite porphyroblasts that were formed during the last stages of the greenschist facies event and shortly after. By examining the porphyroblasts closely, with the hand lense, one can identify σ- and δ-clasts with top-to-SW sense

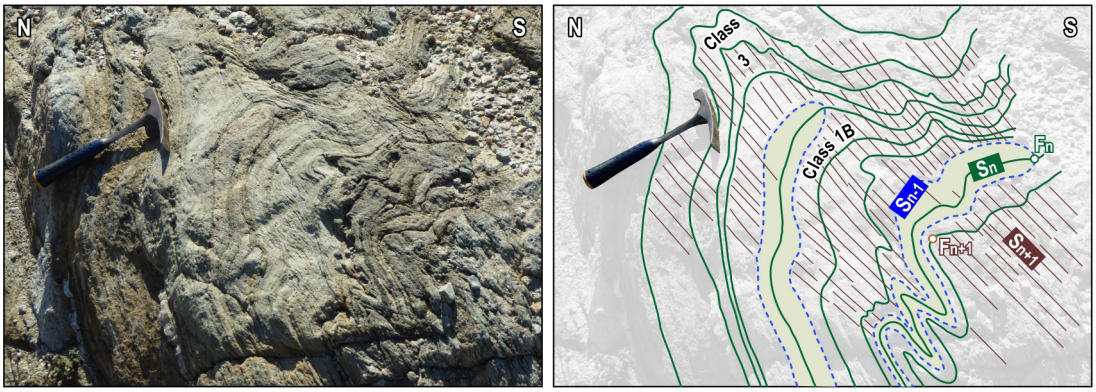

Figure 11
Folding of Dn fabric by Dn+1 and development of Sn+1 axial planar cleavage.

Stop 1.4.a & b: Lithology, protolith of metamorphic rocks and deformation structures of the meta-volacanosedimentary sequence of NEAU.
(1.4.a) 38°03'60"N, 23°54'21"E
(1.4.b) 38°03'57"N, 23°54'38"E

Continue driving to Nea Makri and park right on the road, 50 m before the Stop 1.4.a (Fig. 10). Go on foot to Stop 1.4.a to the left side of the road and then walk along the dirt road to the Stop 1.4.b to see the following interesting structures in the metavolcanosedimentary sequence.

of shear (Fig. 13a). There are also post-tectonic idiomorphic porphyroblasts growing over the Sn main foliation, with no pressure shadows or foliation deflection. Not more than 10-15 meters further up the road, a σ-clast formed from a boudinaged quartz vein, is indicating top-to-SW sense of shear (Fig. 13b). In 15-20 meters, a large lensoid metabasite block can be observed surrounded by schists (Fig. 13c). This belongs to a metabasite layer that can be traced for hundreds of meters, which has been boudinaged in the macro-scale.

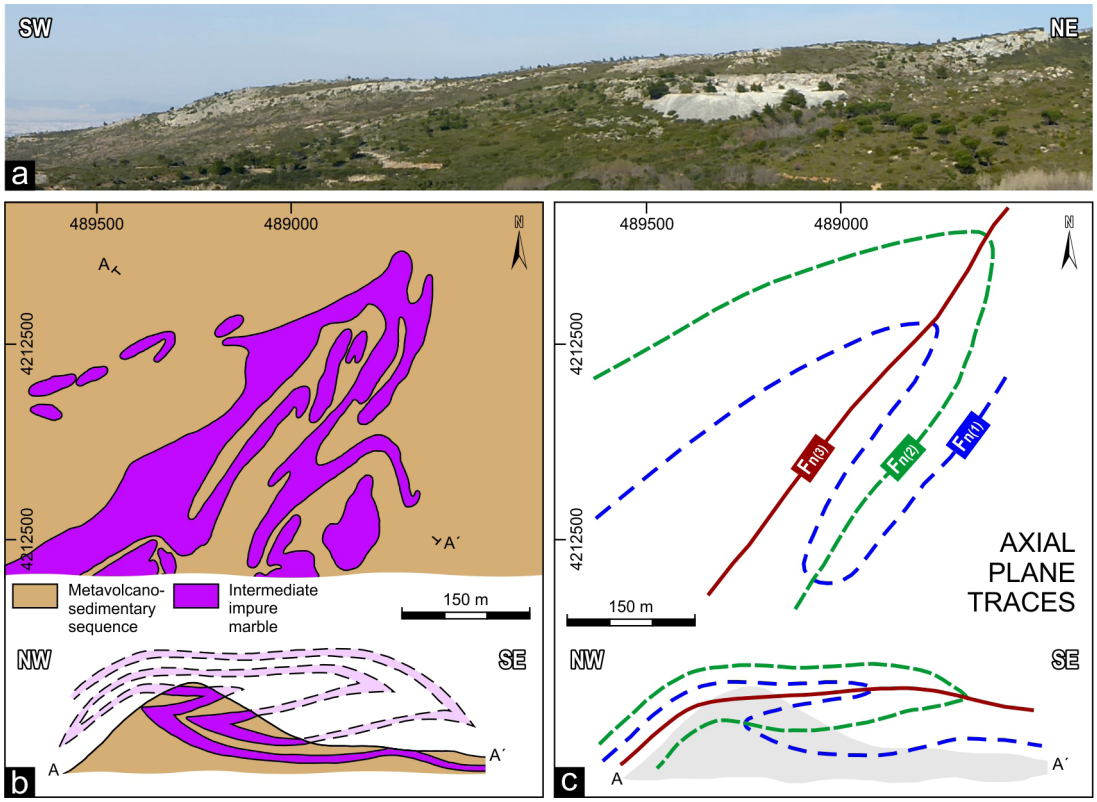

Figure 12
Three superimposed events of km-scale isoclinal folding during Dn, in the blue-grey marble layer.

At about hundred meters, a metaconglomerate layer appears along the road (Fig. 13d). The clasts have an oblate shape revealing that significant flattening has taken place. Most of them are oblique to the foliation and indicate top-to-SW sense of shear. Continue further up to stop 1.4.b. A mesoscopic scale isoclinal fold in a metabasite layer can be observed (Fig. 13e). In the inverted fold limb, a lensoid quartz vein is back-rotated towards the NE into parallelism with the sub horizontal foliation. At the vein wall the foliation is dragged almost at right angles with the foliation, revealing the original relationships (Fig 13f). Hundred meters further ahead (Stop 1.4.b), a ~20 meters thick metagranitoid layer is exposed. This represents the upper part of the metagranitoid rocks of stop 1.6 (see following stops). A layering of metamorphic origin can be observed, formed by alternating relatively thinner (2-15 cm) biotite + chlorite rich layers and quartz + feldspar rich layer. In few places this metamorphic layering is folded isoclinally during Dn (Fig. 13g). Late stage en-echelon array of rotated veins indicates dextral shear (top-to-NE, Fig. 13h) but this is only the 1st set of two conjugate arrays that are observed elsewhere.

Stop 1.5: Sheath folds and eye-shaped outcrop patterns.
38°04'02"N, 23°54'12"E

Continue driving on the asphalt road to Nea Makri, up to the Stop 1.5 (Fig. 10). The outcrop is exposed at the left side of the road. 100 meters ahead there is a parking lot right on the road. Park and return to the Stop 1.5 on foot. On the road cliff, that is almost 10 meters high, metabasic rocks alternating with quartz rich layers (Fig. 14a) represent the earliest generations of quartz-veins which have been fully parallelized to the main Sn foliation. An intense Ln stretching lineation is easily observed on the Sn foliation surfaces (Sn 18/245) constantly trending NE-SW (Ln 255/16). A grate number of micro- and meso-scale isoclinal recumbent Fn folds also occur with their axial planes parallel to the Sn main schistosity (Fig. 14b). In most cases the hinge lines are parallel or sub-parallel to the stretching lineation but there are also cases where the hinge line gradually changes orientation until it is perpendicular to the stretching lineation (Fig. 14d). Sections through

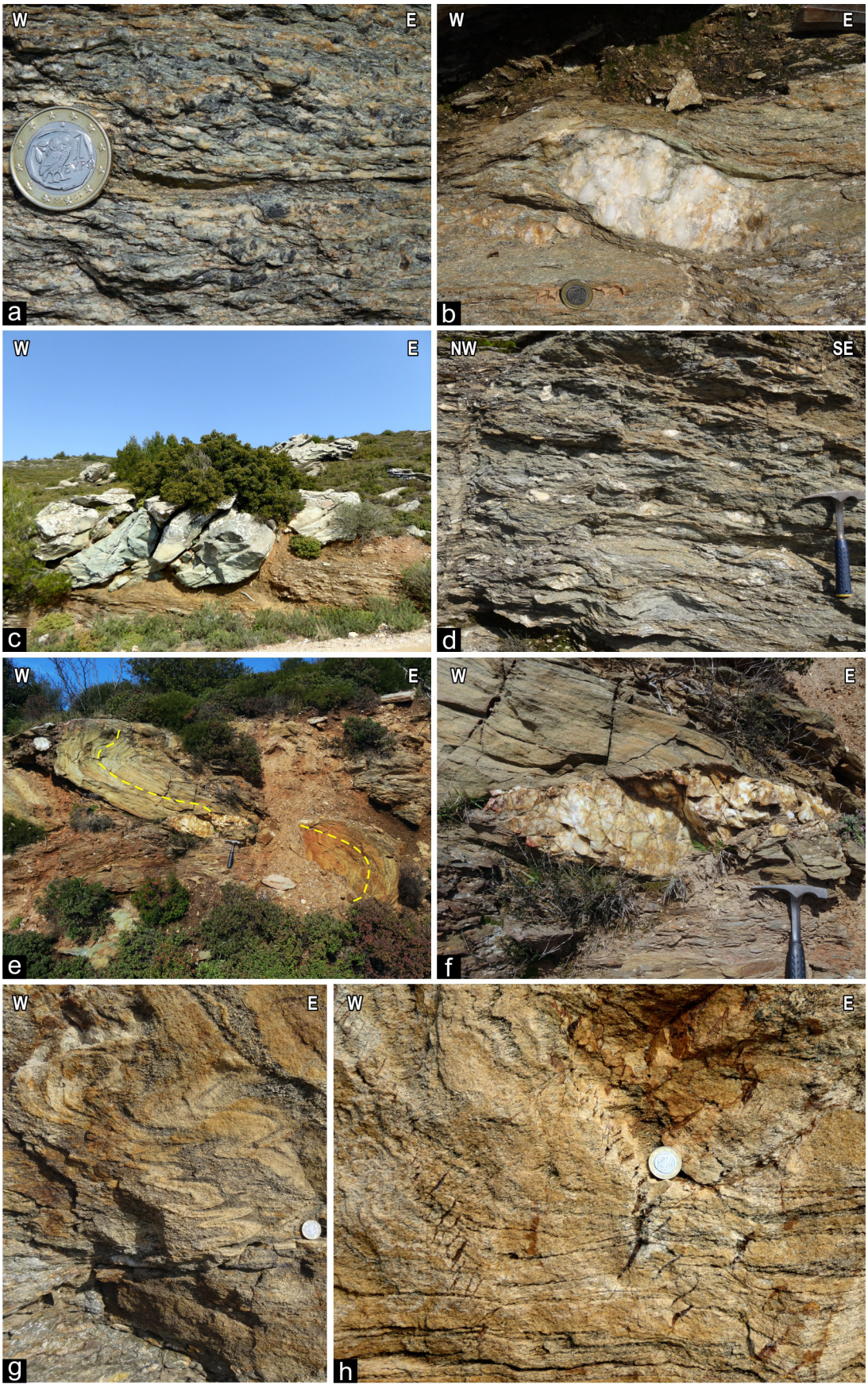

Figure 13
Late- to post-tectonic pyrite porphyroblasts, boudinaged quartz vein, metaconglomerate layer, mesoscopic and microscopic scale isoclinal Fn folds and late stage en-echelon array of rotated veins.

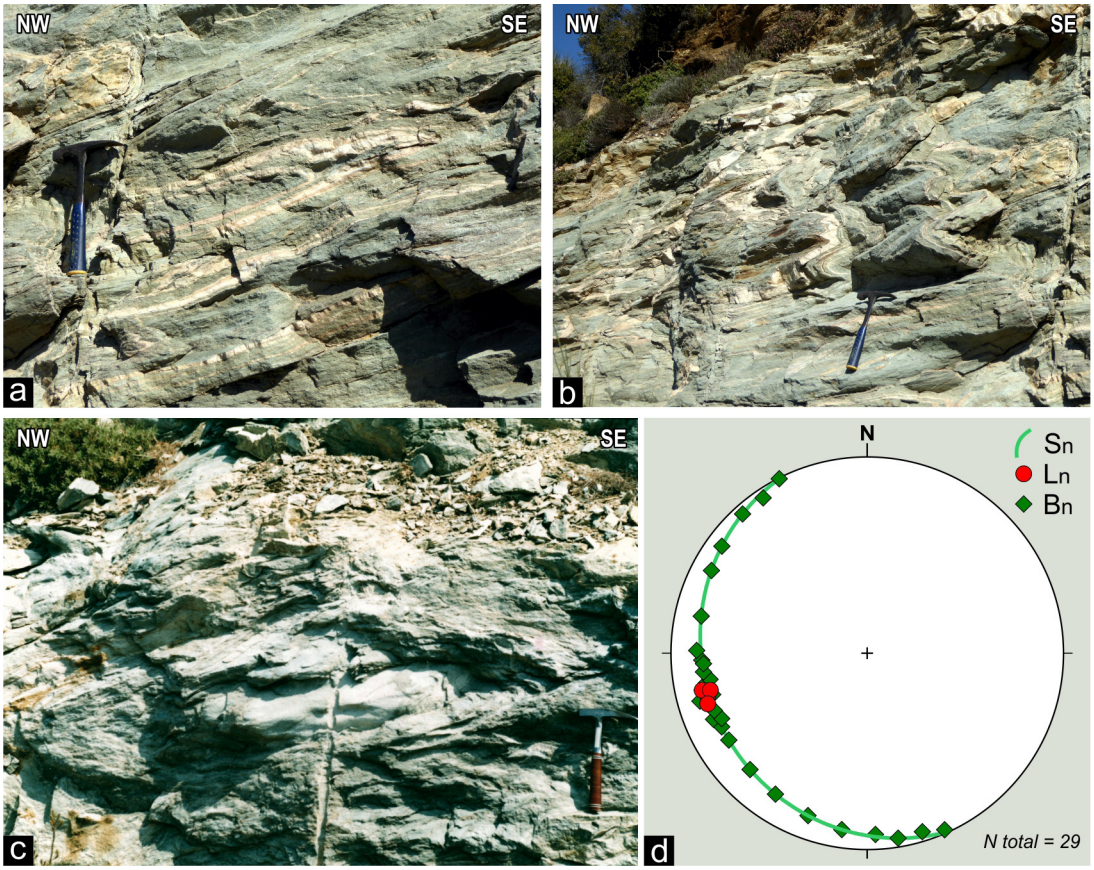

Figure 14
Sheath folds in high strain zones within the meta-basic rocks of NEAU.

these folds resemble Type 1 fold interference patterns and illustrate the characteristic eye-shaped outcrop pattern of sheath folds (Fig. 14c). This rotational behavior of fold hinges is associated with high strain zones in non-coaxial flow where the transport direction coincides with the stretching lineation.

Stop 1.6: Metagranitoid rocks within the meta-volacanosedimentary sequence of NEAU. 38°03'55"N, 23°54'46"E

Continue driving to Nea Makri up to the Stop 1.6 and use the parking area on the right side of the road. On the road cliff at the left side of the road, 1,5 meters thick layer of a quartzofeldspathic rock is interlayered within mica-chlorite schists (Fig. 15a). It extends for several hundred of meters to a few kilometers and it is also cropping out in other places around Penteli Mt., many kilometers away from Stop 1.6. The mineral assemblages of the Sn main foliation consist of K-feldspar + albite + quartz + muscovite + chlorite + biotite + titanite and the fabric appears strongly mylonitic. A lot of σ-type or stacked and rarely δ-type porphyroclasts, about 5 to 10 mm in size, in sections parallel to Ln stretching lineation, show a top-to-SW sense of shear (Fig. 15b&c), but rarely the opposite sense can be also observed.

According to Liati et al. (2013) this rock-type is characterized as an I-type pluton metagranitoid. U–Pb SHRIMP zircon dating showed that crystallization took place in two successive stages, at 255±3 and 246±2 Ma. Based on the new data the authors suggest a rift-related geotectonic setting for the formation of the magmatic protoliths.

Stop 1.7: View of isoclinal macro-folds and underground quarrying in the Penteli Mt. 38°04'20"N, 23°55'08"E

The outcrop locations of Stops 1.7 and 1.8 as well as characteristic locations mentioned in the text, are shown on a Google Earth image in Fig. 16.

Continue driving to Nea Makri. Park at the beginning of the dirt road that leads to the Stop 1.7 and walk up to the top of the hill. Looking towards the southeast to the hill of Mavrinora, the marble overlies the meta-volcanosedimentary sequence. A thick layer of isoclinally folded

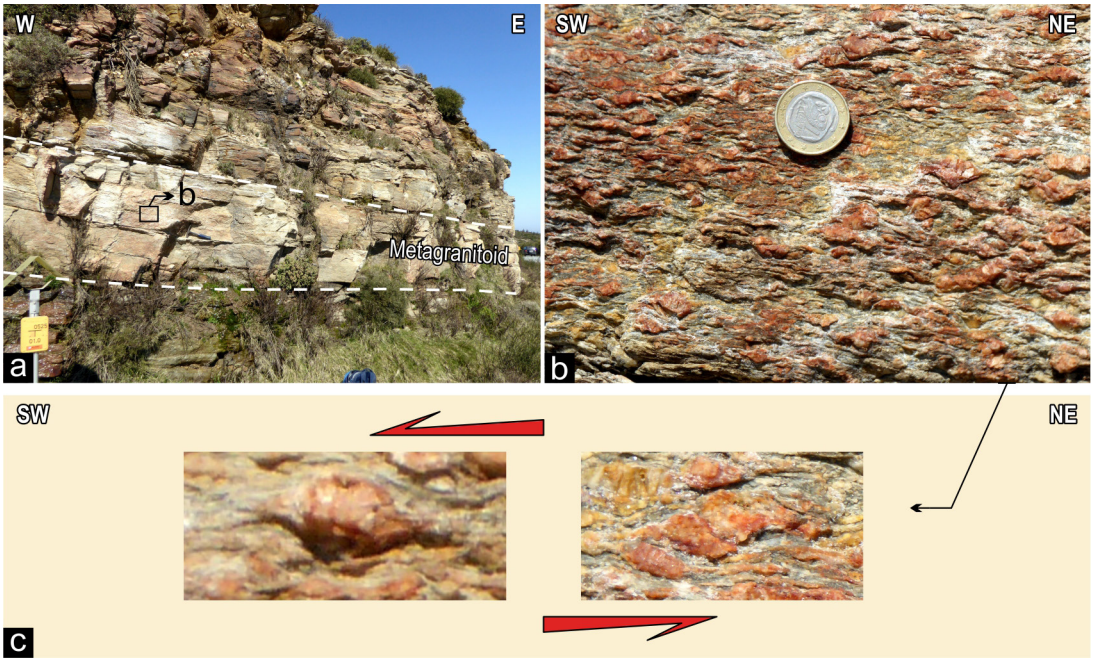

Figure 15
Metagranitoid rocks within the metasediments of NEAU, which exhibit a strong mylonitic foliation including σ-type, δ-type and stacked porphyroclasts.

blue-grey marble is intercalated within the upper part of the meta-volcanosedimentary sequence, forming an asymmetric recumbent macro-fold (including a synform and an antiform) with thickened hinges and attenuated limbs (Fig. 17.a). The orientation of the macro-fold axes is NE-SW, as in other places (see Stop 1.3.b) and they are the result of Dn deformation event. The axial planes, which are identical to the Sn main foliation, are almost flat lying (130/15) and they are verging southeast. The asymmetry and vergence of these hundred meters-scale folds were used by Lozios (1993) to determine the km-scale and first-order tectonic macrostructure of NEAU, during the Dn (and probably Dn-1) syn-metamorphic deformation event. The sketch of Fig. 17.b illustrates the location of the second order isoclinal macro-folds in Mavrinora hill, in respect to the first order structures. Note that the orientation of the isoclinal macro-fold axes is identical to the orientation of the meso- and micro-scale isoclinal Fn folds and parallel to the Ln stretching lineation, which indicates the direction of tectonic transport (see also Stop. 1.5). The existence of large-scale sheath folds may be the explanation to the above observation, as Lozios (1993), suggested for the Dn macro-structure of NEAU, based on vergence and reversals in the polarity of structural facing.

From the same Stop, looking towards the northwest to the eastern slopes of Dionisovouni hill, a large marble quarry is visible due to deforestation and quarrying activity (Fig. 18a). The exploitation of marble takes place to the lower part of the marble of NEAU, where the world-famous "Dionyssos-Pentelicon" marble is produced. Noting that in the quarry area the marble is underlying the schists and metabasite of the meta-volcanosedimentary sequence, as well as the marble layer, because it is located at the reverse limb of a large-scale isoclinal macro-fold (Fig. 18a&b). A few years ago, quarrying was performed on 9 surface and 2 underground sites, using pillared chamber mining method. Today, due to environmental restrictions, only underground quarrying is allowed.

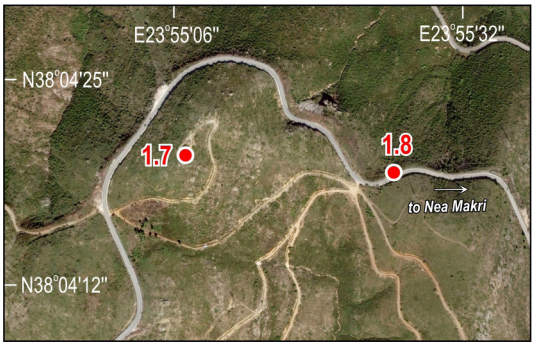

Figure 16
Location of Stops 1.7 and 1.8 on a Google Earth image.

Stop 1.8: Dense Sn+1 crenulation cleavage in calc-schists of NEAU.
38°04'18"N, 23°55'24"E

Continue driving to Nea Makri and park right on the dirt road 80 m before the Stop 1.8 (Fig. 16).

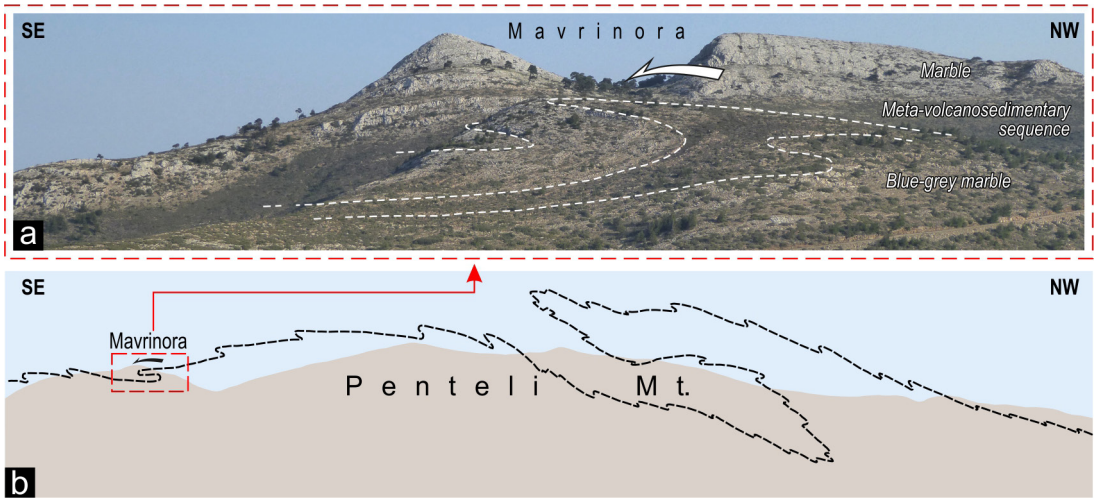

Figure 17
Second order, southeast verging, Fn isoclinal macro-folds and their tectonic position to Penteli Mt. first order tectonic macro-structure.

Go on foot to the stop and study the outcrop with great caution because passing vehicles cannot see you. On the 5 meters high road cliff, calc-schists are exposed with common mineral assemblage calcite + muscovite + chlorite + quartz + albite + chloritoid. The Sn foliation is strongly folded and a densely Sn+1 axial planar crenulation cleavage is developed (Fig. 19a&b). In several cases, the older Sn foliation is almost parallel to the new Sn+1 cleavage and can only be observed in isolated fold hinges. Sn (070/40) and Sn+1 (090/30), intersect creating a NW-SE (140/25) Ln+1 intersection/crenulation lineation. Fn+1 fold axes in this location have similar orientation (Fig. 19c). In

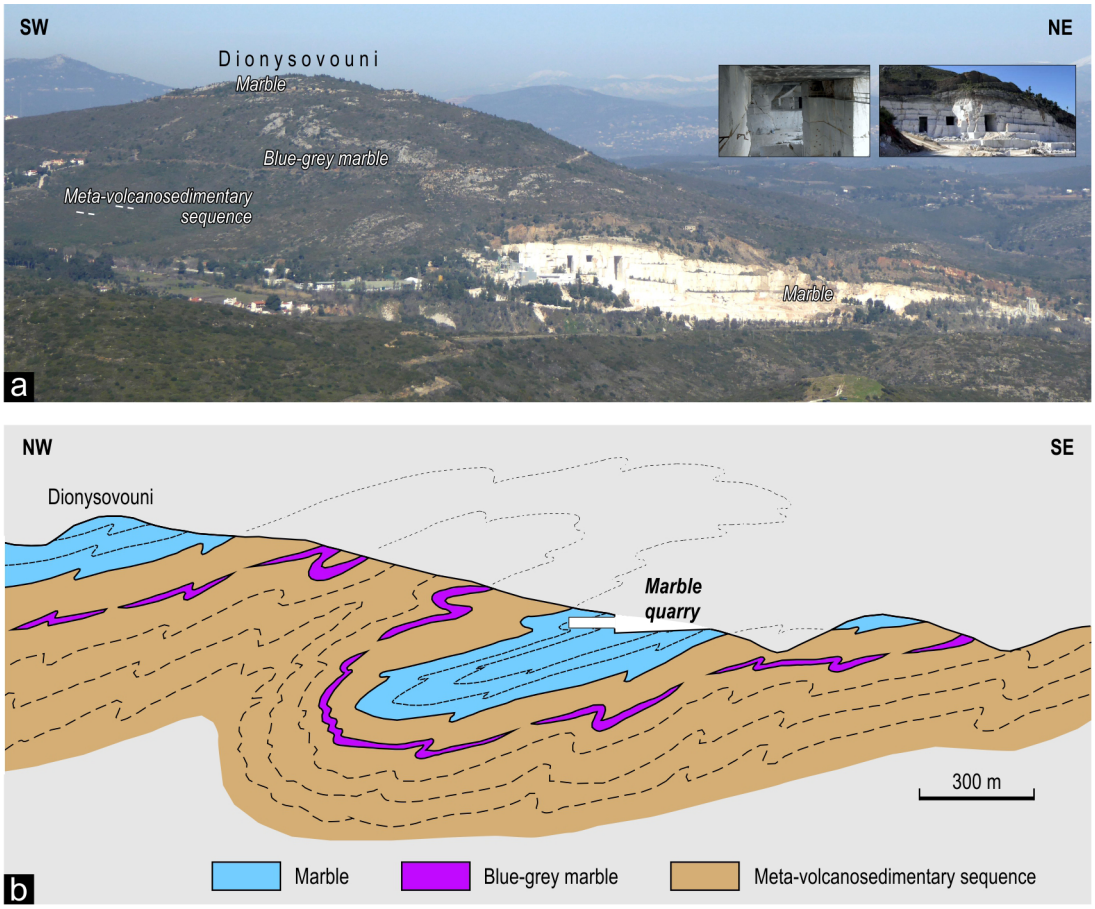

Figure 18
Underground marble quarrying in Dionysovouni area, where the famous "Dionyssos-Pentelicon" marble is being exploited.

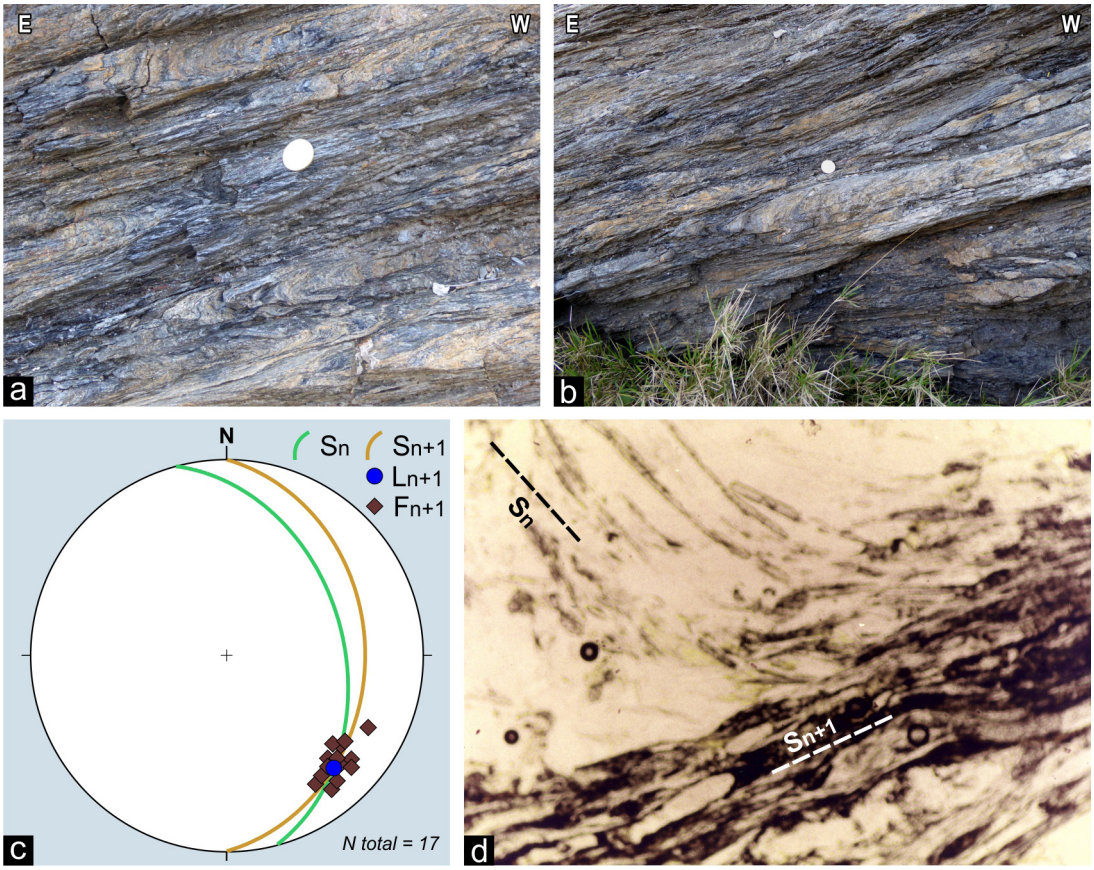

Figure 19
Morphological and geometrical features of the Dn+1 crenulation cleavage in calc-schists of the meta-volcanosedimentary sequence of NEAU.

thin sections the Sn+1 cleavage is smooth (rarely rough), parallel and discrete (rarely gradational) along which the Sn minerals are commonly reoriented. In some cases, small scale recrystallisation of quartz, muscovite and chlorite occurs (Fig. 19d).

Excursion 2: Marathon reservoir, Ramnous archaeological site and Varnavas village.

This excursion includes four short walks and several point observations along foot paths and dirt or asphalt roads. The lithological and petrographical differences and the tectonic contact between AGU and NEAU, as well as the tectonic structures forming the fabric of AGU and NEAU are shown, described and discussed.

Stop 2.1: The dam and the Marathon reservoir. 38°10'05"N, 23°54'22"E

The outcrop locations of Stops 2.1 and 2.2 as well as characteristic locations mentioned in the text, are shown on a Google Earth image in Fig. 20.

The first stop of the 2nd excursion (Stop 2.1) is located at the dam of the artificial lake of Marathon (or Marathonas). The lake is a water supply reservoir formed by the construction of the Marathon Dam in the early 1930s to cover the growing needs of the capital for water after the huge immigration wave that followed the Asia Minor War (1919-1922). It is an arch dam (Fig. 21a&b) made of concrete (with an external cladding of white Pentelikon marble) which is curved upstream to transmit the major part of the water load to the abutments. The dam has been founded on the marble and the metabasite (meta-volcanosedimentary sequence) of NEAU at the junction of Charadros and Varnavas torrents. Both abutments rests on competent rocks and more specifically the southern one on the metabasite (Fig. 21b) and the northern one partly on the overlying marble and partly on the underlying metabasite (Fig. 21a). The reservoir has overwhelmed mainly the impermeable metasediments of AGU as well as the low-angle normal fault between the two units (see the Geological Map).

Figure 20
Location of Stops 2.1 and 2.2 on a Google Earth image.

Stop 2.2.a-c: The normal fault between AGU and NEAU and the available kinematic data. Lithological and petrographical differences between AGU and NEAU.
(2.2.a) 38°11'01"N, 23°54'35"E
(2.2.b) 38°11'14"N, 23°54'31"E
(2.2.c) 38°11'19"N, 23°54'27"E

From Marathon Dam drive towards the Marathon town and in about 2 km at the entrance of the Vothonas small village turn left towards Grammatiko town. In about 400 m turn left to the dirt road leading to the small church of Agia Paraskevi. Park and walk along the dirt road to the Stop 2.2.a (about 700 m). At the right side of the road the underlying meta-volcanosedimentary sequence and the overlying marble are dipping WNW (285/55). As detailed mapping revealed, in this area, there are at least two repetitions of the lithologies due to the isoclinal folding in the macro-scale.

At the Stop 2.2.a, a moderate angle normal fault has brought in contact the marble of the underlying NEAU (footwall) and the schists of the overlying AGU (hanging wall, Fig. 22a). The fault surface dips 292/45 but more to the north it bends to the east and dips 345/47. The same geometry is also followed by the Sn foliation of the footwall rocks (marble, schists and metabasite) of NEAU (see the Geological Map). Cataclastic deformation accompanied by massive fluid infiltration and extensive ankeritization has taken place along the fault zone. Slickenlines or other kinematic data are very rare because the fault surface is strongly weathered. In a few places badly preserved slickenlines and fault surface corrugations show a dip slip normal movement (Fig. 22b&c).

On the road cliff and just below the fault surface flanking structures can be observed on the marble of NEAU (Fig. 22d&e). They represent shear band - reverse type flankings, showing a top-to-SW sense of shear (Passchier 2001, Grasemann et al. 2001, 2003).

Continue walking along the dirt road to the Stop 2.2.b (about 500 m). Along the route and on the right side of the road the schists and quartzite of AGU are exposed (Fig. 23a). The common mineral assemblage for schists includes quartz + muscovite + chlorite ± albite ± Na-amphibole ± epidote ± calcite ± biotite ± titanite. The schists are very rich in Na-amphibole (Fig. 23a) whereas actinolite is very rare. The Sn main schistosity is dipping 080/38 and the Ln mineral or stretching lineation 052/30 (Fig. 23d). The Fn+1 fold axes as well as the Ln+1 intersection/crenulation lineation, are plunging 10-20 to the NW (Fig. 23a&d).

At Stop 2.2.b a massive metabasite block within the schists is cropping out (Fig. 23b). The typical mineral assemblage for this type of rock includes albite + chlorite + epidote + actinolite ± Na-am-

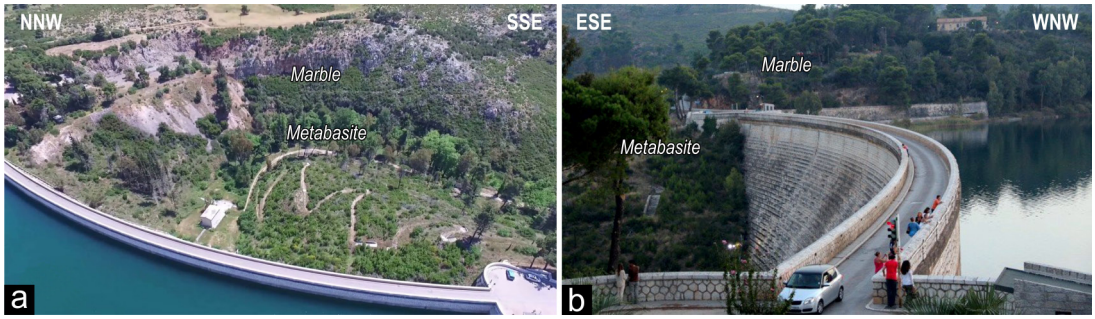

Figure 21
The arch dam of Marathon founded on the metabasite and marble of NEAU. The reservoir overwhelms the metasediments of AGU.

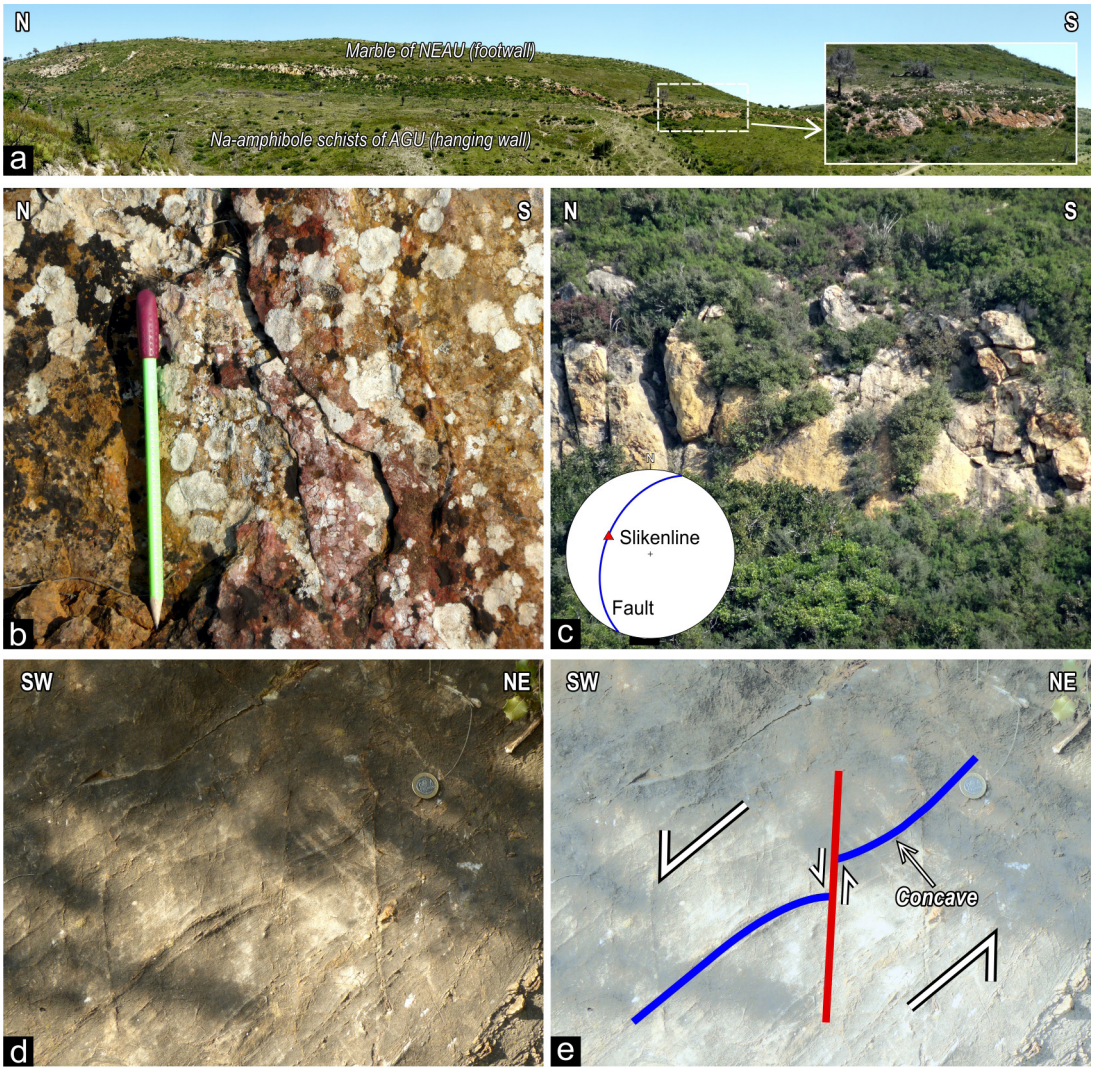

Figure 22
The normal fault between AGU and NEAU and the available kinematic data.

phibole ± muscovite ± biotite ± quartz ± calcite ± titanite. Most samples are very rich in Na-amphibole (Fig. 23b), which is often replaced by actinolite.

Walk to Stop 2.2.c (about 300 m). In a plowed field a small outcrop of metachert marble appears (Fig. 23c) as a distinct layer within the schists of the AGU. Below the marble a small outcrop of serpentinite is also exposed. Such rock types are observed as tectonic slices with varying dimensions in between the metamorphic rocks both NEAU and AGU in many places. The common minerals are serpentine, talc and relic pyroxene.

Stop 2.3: Fn and Fn+1 folds in metachert marble layers at the base of the neritic platform of NEAU.
38°10'46"N, 24°01'22"E

The outcrop locations of Stops 2.3 and 2.4 as well as characteristic points and locations mentioned in the text, are shown on a Google Earth image in Fig. 24.

Return to Vothonas village and follow the road to Marathon city (about 7 km) and then the road to Kato Souli Village (about 7,5 km). Continue the road to Ancient Ramnous archaeological site and about 1,5 km after Kato Souli (point P1, Fig. 24), park on the left side of the road. Walk on foot up to Stop 2.3, on the slopes of the small hill Agrilia. At the contact between the overlying marble and the underlying meta-volcanosedimentary sequence of NEAU, an intensely folded cherty marble is cropping out. In N-S oriented sections, the Fn isoclinal recumbent and long-limbed folds are impressively exposed, where at least two or three coaxial and co-planar refolding stages can be recognized (Fig. 25a). The limbs are usually strongly thinned or totally detached while the hinges are very thickened. In most cases the folds appear as

intrafolial and rootless folds with strongly attenuated limbs. They are usually co-planar tight folds with variably oriented axes and sheath folds with arcuate hinges (see inlet in Fig. 25a), like those described at Stop 1.5 on the southern slopes of Penteli Mt. The main Sn foliation is dipping about 70° to the West (274/70), the Ln stretching lineation is trending NE-SW (228/62) but the plots of the Fn fold axis in the Schmidt net are usually distributed around the stretching lineation or rarely along the axial plane, which coincides with the main foliation (Fig. 25b).

In E-W oriented sections, mainly along vertical joints, the Fn+1 folds are exposed. They are formed by the folding of the Sn main foliation and represent upright or inclined, open to closed, symmetrical folds, with fold axes that plunge 330/10 or 180/05 (Fig. 25c&d). Occasionally, in small-scale folds an Ln+1 crenulation lineation is formed.

Stop 2.4: High angle normal neotectonic faults. 38°11'12"N, 24°02'26"E

Return to point P1 and continue driving north. At point P2 turn right to Agia Marina Port and in about 700 meters park to the right of the road. Walk to Stop. 2.4 (see Fig. 24). In the area between the settlement of Avra and Agia Marina Port NW-SE horsts and half-grabens are formed. Their NE margins bounded by high angle normal faults (see Fig. 24 and the Geological Map), parallel to the Southern Evoikos Gulf active submarine faults. The fault scarp is about 2-3 meters high (Fig. 26a) and scree with a thickness of about 5-10 meters cover the fault trace. A 30-40 cm thick cataclasite has been developed along the fault surface, mainly

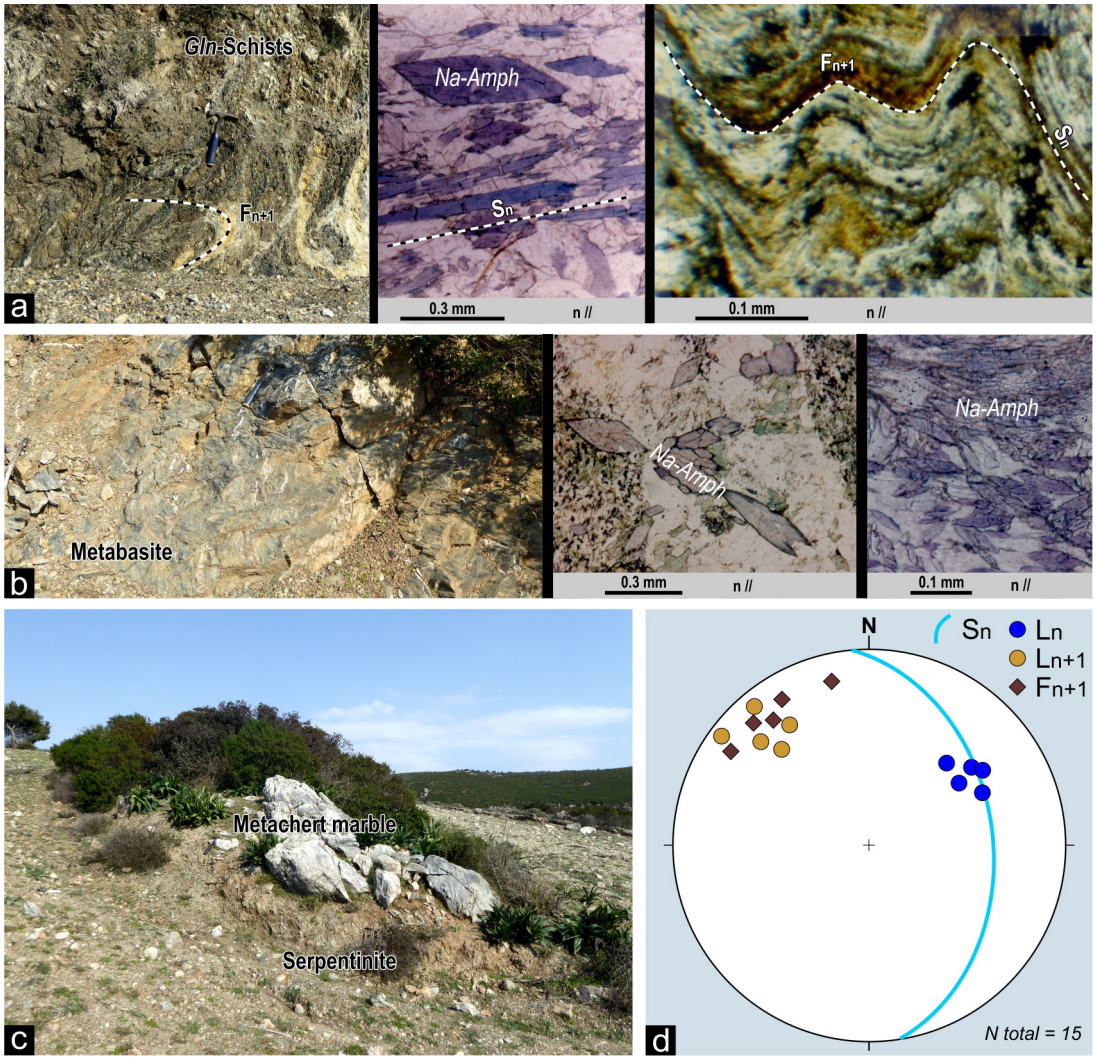

Figure 23
Lithological, petrographical and structural data of Agios Georgios Unit.

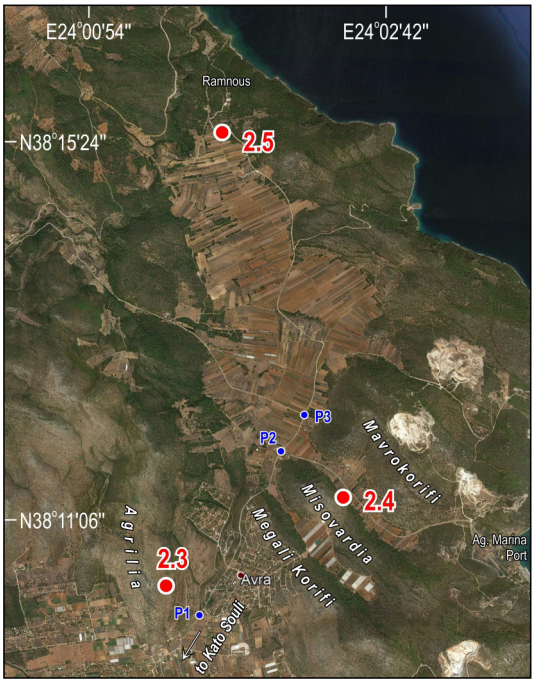

Figure 24
Location of Stops 2.3 and 2.4 on a Google Earth image.

fault breccia or microbreccia (Fig. 26b). The fault surface is dipping NE (035/75) and small-scale corrugations and slickenlines (029/74), reveal a dip-slip normal movement (Fig. 26c&d).

Stop 2.5: Ancient Ramnous archaeological site and Fn macro-folds.
38°12'56"N, 24°01'42"E

Return to point P2 and continue driving north to Stop 2.5. Park at the entrance to the archaeological site of Ramnous (or Rhamnous) and follow on foot the dirt road to the ruins of the ancient town (Fig. 27a). Ramnous is an ancient Greek town, located on the NE Attica coast, about 55 kilometers from Athens. It was named after the local prickly bush called ramnos and was the sanctuary of Nemesis in ancient Greece. Excavations have brought to light the most important sanctuary of Nemesis in ancient Greece, the fortress, public buildings, remains of houses and many grave enclosures. The fortified settlement of Ramnous was of strategic importance to Athens in the Archaic and Classical eras because it guarded over Euripos and two small harbors that provided shelter off the east coast of Attica to southbound ships.

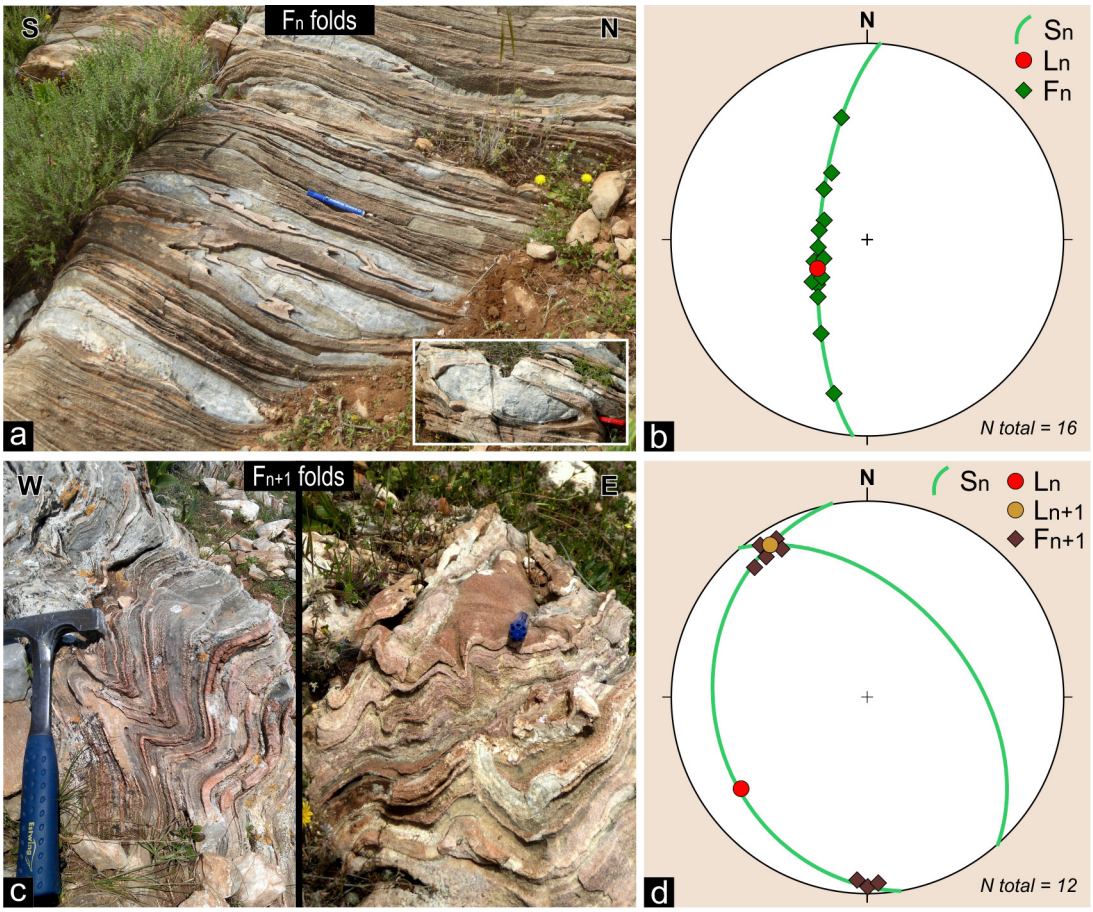

Figure 25
Impressive exposures of the Fn and Fn+1 folds on the metachert marble layers at the base of NEAU.

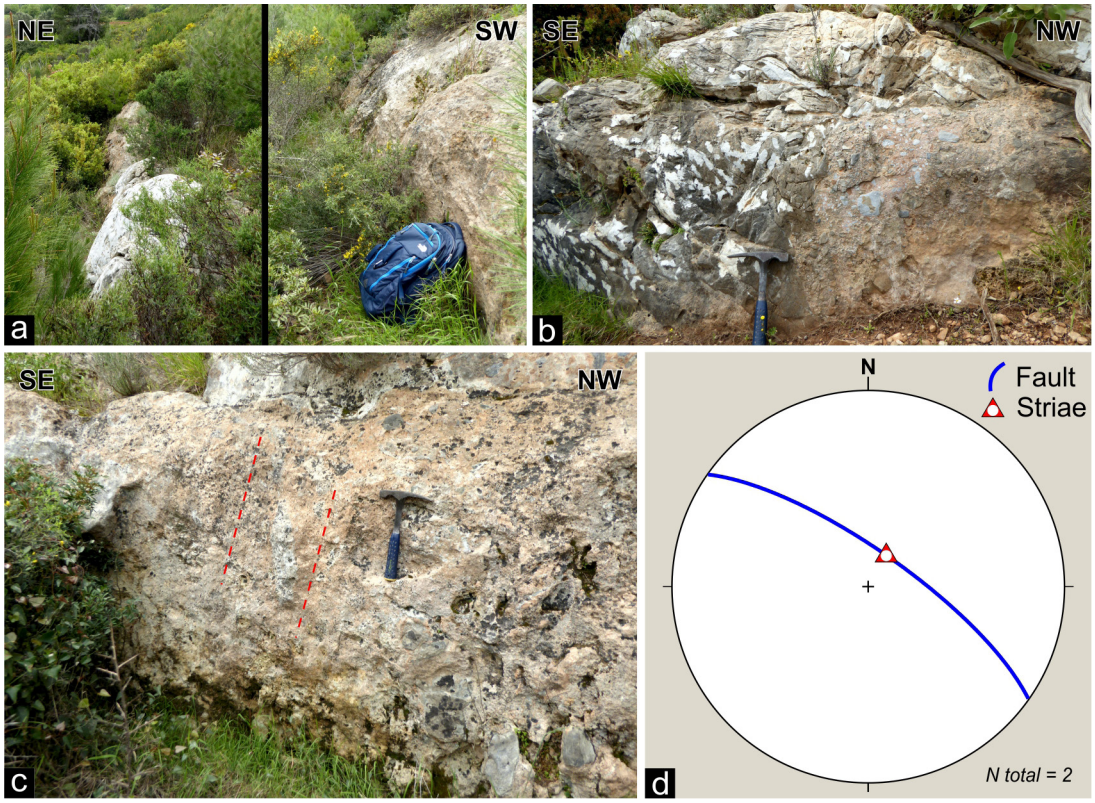

Figure 26
IHigh angle fault surface, cataclasites, dip-slip slickenlines and small-scale corrugations.

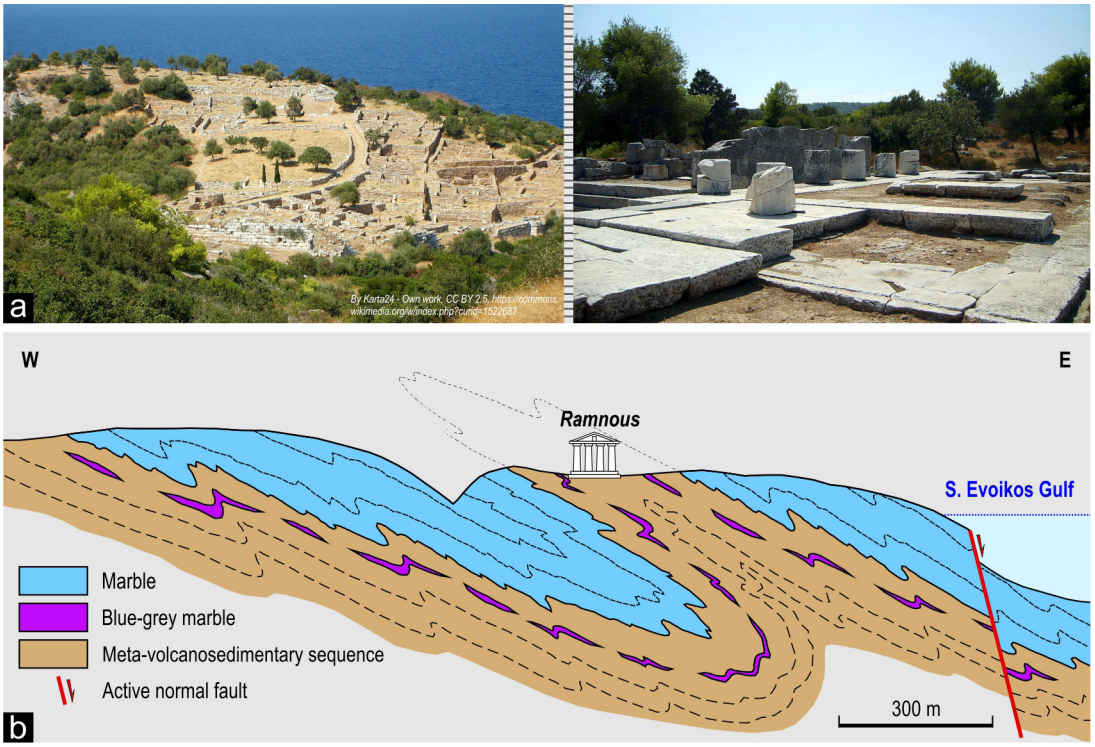

Figure 27
The ruins of the ancient Ramnous town are sited on the schists of NEAU, in the core of an isoclinal Fn macro-fold.

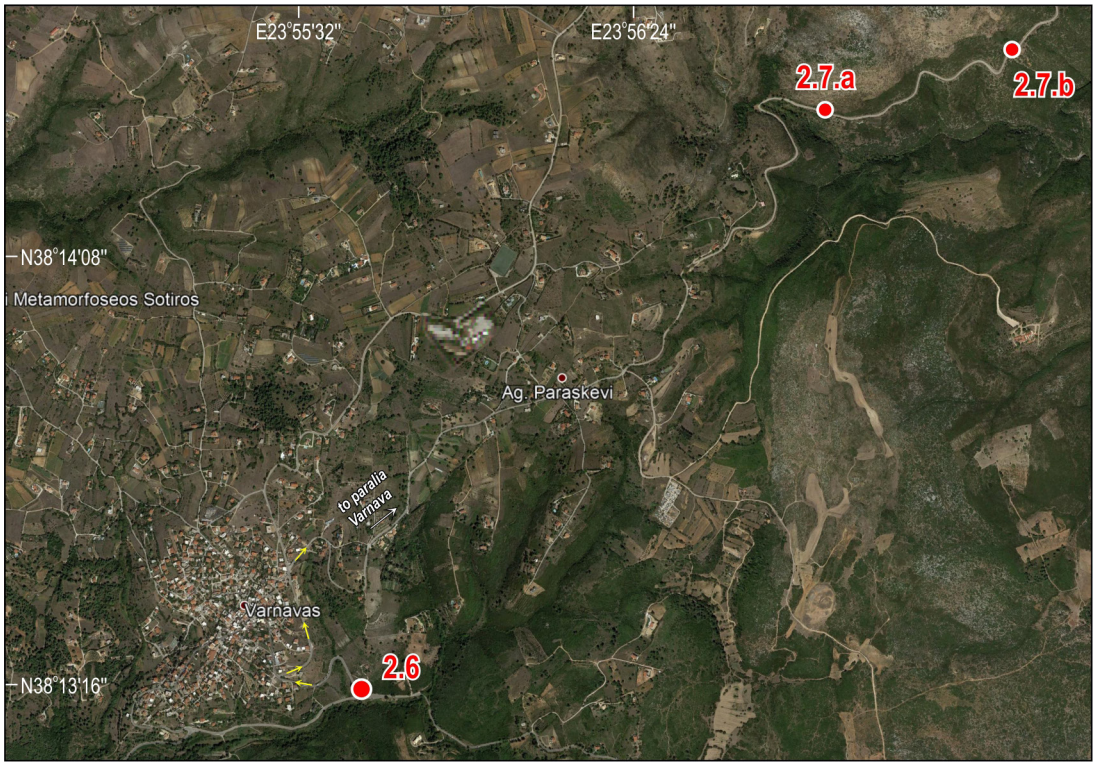

Figure 28
Location of Stops 2.6, 2.7 and 2.8 on a Google Earth image.

During the Peloponnesian war, and after the Spartans occupied the fort of Dekelia located north of Athens, Rhamnous provided safe passage of food supplies that came from Evia Island.

The ancient town of Ramnous is built on the schists and the blue-grey marble layer of the me-

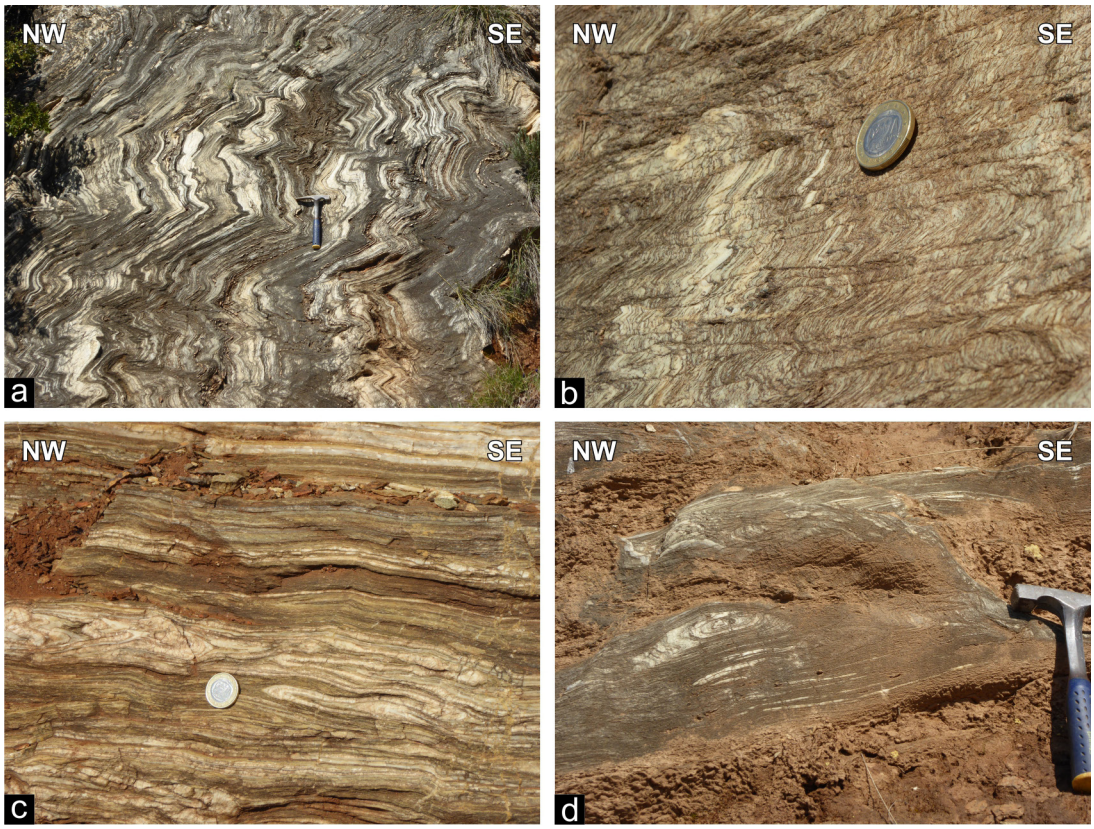

Figure 29
Fn+1 folds and Sn+1 axial planar cleavage, Fn isoclinal folds and interference patterns formed by the two sets of folds in the blue-grey and metachert marble of NEAU.

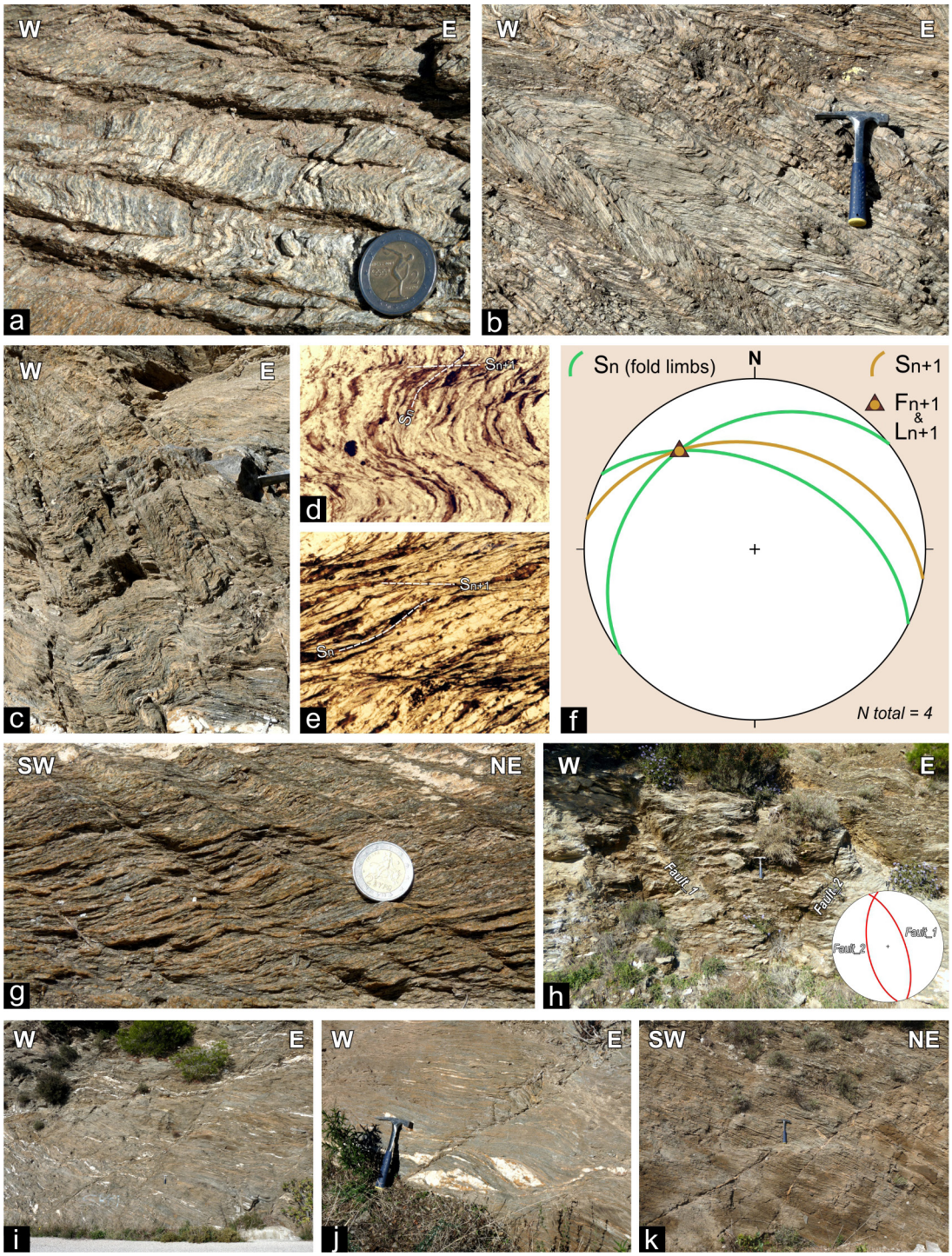

Figure 30
Fn+1 axial planar cleavage, top-to-NE shearbands and high-angle normal faults in quartz-mica schists of NEAU.

ta-volcanosedimentary sequence of NEAU, at the core of an Fn inclined isoclinal macro-fold. So, at the east of the Ramnous ruins the marble of NEAU overlying the schists while at the west the schists overlying the marble (Fig. 27b). The whole macro-structure is interrupted to the east by the neotectonic active faults of Southern Evoikos Gulf (see also the Geological Map).

Stop 2.6: Fn and Fn+1 folding, Sn+1 crenulation cleavage and fold interference patterns in the blue-grey marble of NEAU.
38°13'15"N, 23°55'41"E

The outcrop locations of Stops 2.6, 2.7 and 2.8 as well as characteristic points and locations men-

tioned in the text, are shown on a Google Earth image in Fig. 28.

Return to point P3 (Fig. 24) and turn right on the asphalt road to the town of Grammatiko. Continue driving towards the town of Varnavas up to Stop 2.6 at the entrance of the town (Fig. 28). On the road cliff the blue-grey and metachert marble of NEAU is exposed. Numerous mesoscopic scale Fn+1 folds can be identified (Fig. 29a). They are typically NW-SE upright chevron folds or box folds (fold axes ~310/24). A dense Sn+1 axial planar crenulation cleavage is developed in many cases where the Sn main foliation is intensely folded (Fig. 29b). Small scale NE-SW Fn recumbent isoclinal folds can also be observed within the main Sn foliation (Fig. 29c). More specifically, the refolding of isoclinal Fn folds by Fn+1 folds creates intermediate 1-01 type interference patterns (Fig. 29d, Ramsay 1967, Grasemann et al. 2004).

Stop 2.7.a & b: The Fn+1 refolding, the Sn+1 axial-planar cleavage and high angle normal faults in the mica schists of NEAU.
(2.7.a) 38°14'25"N, 23°56'56"E
(2.7.b) 38°14'33"N, 23°57'22"E

Continue driving NNE following the signs to Paralia Varnava up to Stop 2.7.a (see Fig. 28) and park your car. Walking along the road from Stop 2.7.a to Stop 2.7.b, quartz-mica schists are exposed on the road cliff. A strong crenulation cleavage is ubiquitous, where the Sn main foliation is folded and a Sn+1 axial planar cleavage is developed. Spacing between the cleavage domains varies from 1-2 cm (or less), up to 10-20 cm and rarely even more. The Fn+1 folds are plunging inclined, with the axial plane dipping 010/38 and the fold axis plunging 323/28. The minerals of the Sn main schistosity are usually reoriented towards the phyllosilicate-rich Sn+1 cleavage planes that bound the quartz-rich microlithon. Shear bands deform the Sn+1 cleavage, as well as the Sn main foliation, showing a top-to-NE sense of shear.

Numerous normal faults crosscut all the previous structures. They represent a conjugate system where the 1st set is dipping 070/65 and the 2nd 260/60. In some cases, in vertical cross-sections or between splay faults ramp-flat-ramp geometries and overlap zones can be observed (Fig. 30i,g&k).

REFERENCES

Baziotis, I., Mposkos, E., Perdikatsis, V., 2004. Pre-alpine migmatitic rocks and acid to intermediate orthogneisses in Pentelikon Mountain (NE Attica, Greece). Bulletin of the Geological Society of Greece XXXVI, 542–551.

Baziotis, I., Proyer, A., Mposkos, E., 2009. High-pressure/low-temperature metamorphism of basalts in Lavrion (Greece): implications for the preservation of peakmetamorphic assemblages in blueschists and greenschists. European Journal of Mineralogy 21 (1), 133–148.

Baziotis, I., Mposkos, E., 2011. Origin of metabasites from upper tectonic unit of the Lavrion area (SE Attica, Greece): Geochemical implications for dual origin with distinct provenance of blueschist and greenschist's protoliths. Lithos 126, 161–173.

Baziotis, I., Proyer, A., Mposkos, E., Windley, B.F., Boukouvala, I., 2019. Exhumation of the high-pressure northwestern Cyclades, Aegean: New P-T constraints, and geodynamic evolution. Lithos 324–325, 439–453.

Berger, A., Schneider, D.A., Grasemann, B., Stockli, D., 2013. Footwall mineralization during Late Miocene extension along the West Cycladic Detachment System, Lavrion, Greece. Terra Nova 25, 181-191.

Grasemann, B., Stuwe, K., 2001. The development of flanking folds during simple shear and their use as kinematic indicators. Journal of Structural Geology 23, 714–724.

Grasemann, B., Stuwe, K., Vannay, J-C., 2003. Sense and non-sense of shear in flanking structures. Journal of Structural Geology 25, 19–34.

Grasemann, B., Wiesmayr, G., Draganits, E., Fusseis, F., 2004. Classification of Refold Structures. The Journal of Geology 112 (1), 119–125.

Grasemann, B., Schneider, D.A., Stockli, D.F. and Iglseder, C., 2012. Miocene bivergent crustal extension in the Aegean: evidence from the western Cyclades (Greece). Lithosphere, 4, 23-39.

Iglseder, C., Grasemann, B., Rice, A.H.N., Petrakakis, K., Schneider, D.A., 2011. Miocene south directed low-angle normal fault evolution on Kea Island (West Cycladic Detachment System, Greece), Tectonics 30, TC4013, doi:10.1029/2010TC002802.

Katsikatsos, G., Migiros, G., Triantafillis, M., Mettos, A., 1986. Geological structure of Internal Hellenides (E. Thessaly—SW Macedonia, Eu-

boa–Attica–Northern Cyclades Islands and Lesvos). Institute of Geology and Mining Research (IGMR), Athens, Geological and Geophysical Research, Special Issue, 191–212.

Katsikatsos, G., 1990. Geological Map of Greece, Rafina Sheet 1.50.000. Institute of Geology and Mining Research (IGMR), Athens.

Katsikatsos, G., 2002. Geological Map of Greece, Kifissia Sheet 1.50.000. Institute of Geology and Mining Research (IGMR), Athens.

Kessel, G., 1990. Untersuchungen zu Deformation und Metamorphose im Attischen Kristallin, Griechenland. Berliner geowissenschaftliche Abhandlungen., Reihe A, Geologie und Paläontologie, Bd. 126, 150s.

Krohe, A., Mposkos, E., Diamantopoulos, A., Kaouras, G., 2010. Formation of basins and mountain ranges in Attica (Greece): the role of Miocene to recent low-angle normal detachment faults. Earth-Science Reviews 98 (1–2), 81–104.

Lekkas, S., Lozios, S., 2000. Tectonic structure of Mt. Hymittos. Annales Géologiques des Pays Helléniques 38, 47–62.

Lekkas, S., Skourtsos, E., Soukis, K., Kranis, H., Lozios, S., Alexopoulos, A., Koutsovitis, P., 2011. Late Miocene detachment faulting and crustal extension in SE Attica (Greece). Geophysical Research Abstracts 13, EGU2011–13016.

Liati, A., Skarpelis, N., Pe-Piper, G., 2009. Late Miocene magmatic activity in the Attic-Cycladic Belt of the Aegean (Lavrion, SE Attica, Greece): implications for the geodynamic evolution and timing of ore deposition. Geological Magazine 146 (5), 732–742.

Liati, A., Skarpelis, N., Fanning, C. M., 2013. Late Permian–Early Triassic igneous activity in the Attic Cycladic Belt (Attica): New geochronological data and geodynamic implications. Tectonophysics 595–596, 140–147.

Lozios, S. 1990. Microtectonic observations at the metamorphic formations of Varnavas-Ramnounda area (NE Attica, Greece). Bulletin of the Geological Society of Greece 25, 439–453. (In Greek).

Lozios, S., 1993. Tectonic analysis of the metamorphic formations of NE Attica. PhD Thesis, University of Athens, 299 pp. (In Greek). http://hdl.handle.net/10442/hedi/2925

Marinos, G., 1948. Notes on the structure of Greek marbles. American Journal of Science 246, 386–389.

Marinos, G. and Petraschek, W.E., 1956. Laurium. Institute of Geology and Mining Research (IGMR), Athens, Geological and Geophysical Research, Special Issue 1–247.

Passchier, C.W., 2001. Flanking structures. Journal of Structural Geology 23, 951–962.

Papadeas, G., 1970. Zur stratigraphie und Alterstellung der metamorphern Sherien NE von Athen (Marathon). (Zusammenfassung der Ergebnisse). Proceedings of the Athens Academy 44, 10–18.

Papadeas, G., 1973. Zur Geologie der kristallinen Gesteine von Marathon. Bulletin of the Geological Society of Greece X (2), 13–64.

Papadeas, G., 1986. Startigraphy and age of the metamorphic rocks of NE Attica. Bulletin of the Geological Society of Greece XVII, 59–81. (In Greek)

Papanikolaou, D., Bassi, E.K., Kranis, H., Danamos, G., 2004a. Paleogeographic evolution of the Athens basin from upper Miocene to present. Bulletin of the Geological Society of Greece 36 (2), 816–825. (In Greek)

Papanikolaou, D.I., Lozios, S.G., Soukis, K., Skourtsos, E., 2004b. The geological structure of the allochthonous "Athens Schists". Bulletin of the Geological Society of Greece 36 (4), 1550–1559. (In Greek)

Pe-Piper, G., Piper, D.J.W., 2002. The Igneous Rocks of Greece: The Anatomy of an Orogen. Gebrüder Borntraeger, Berlin, 573 pp.

Photiades, A., Carras, N., 2001. Stratigraphy and geological structure of the Lavrion area (Attica, Greece). Bulletin of the Geological Society of Greece XXXIV (1), 103–109.

Ramsay, J.G., 1967. Folding and fracturing of rocks. McGraw Hill, New York, 568 pp.

Seman, S., Soukis, K., Stockli, D.F., Skourtsos, EM., Kranis, H., Lozios, S., 2012. Novel thermochrono-metric techniques applied to the Lavrion Detachment, Lavrion Peninsula, Attica, Greece. Mineralogical Magazine Abstracts 76, 2352.

Seman, S., Soukis, K., Stockli, D.F., Skourtsos, Em., Kranis, H., Lozios, S., 2013. Provenance of metasediments and Miocene exhumation history of the Lavrion Peninsula, South Attica, Greece: A combined structural, (U-Th)/He, and detrital zircon U-Pb study. Geophysical Research Abstracts 15, EGU2013–12605.

Scheffer, C., Vanderhaeghe, O., Lanari, P., Tarantola, A., Ponthus, L., Photiades, A., France, L., 2016. Syn- to post-orogenic exhumation of

metamorphic nappes: Structure and thermobarometry of the western Attic-Cycladic metamorphic complex (Lavrion, Greece). Journal of Geodynamics 96, 174–193.

Skarpelis, N., 2007. The Lavrion deposit: geology, mineralogy and minor elements chemistry. Neues Jahrbuch für Mineralogie Abhandlungen 183/3, 227–249.

Skarpelis, N., Tsikouras, B., Pe-Piper, G., 2008. The Miocene igneous rocks in the Basal Unit of Lavrion (SE Attica, Greece): petrology and geodynamic implications. Geological Magazine 145 (1), 1–15.

Spanos, D., Koukouvelas, I., Kokkalas, S., Xypolias, P., 2010. Patterns of ductile deformation in Attico-Cycladic massif. Bulletin of the Geological Society of Greece 43(1), 368–378.

Xypolias, P., Spanos, D., Chatzaras, V., Kokkalas S., Koukouvelas I., 2010. Vorticity of flow in ductile thrust zones: examples from the Attico-Cycladic Massif (Internal Hellenides, Greece). Geological Society, London, Special Publications 335, 687–714.